



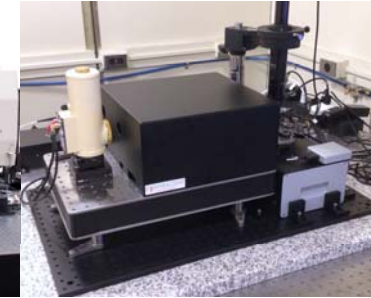
AFM integration with Laser Spectroscopy: Challenges, Solutions, Advantages

Shelaev Artem, application scientist
shelaev@ntmdt-si.com

Product Line

AFM

AFM-Raman / IR / TERS



SOLVER NANO

NEXT / TITANIUM

NTEGRA

NTEGRA SPECTRA II

NTEGRA IR

- Compact desktop AFM/STM for both education and science
- Full set of AFM/STM modes
- High AFM/STM performance
- Closed-loop Scanner

- AFM/STM with exceptional level of automation
- Fast, precise and low-noise closed-loop scanner
- High resolution imaging due to extremely low noise and high stability
- Full set of standard and advanced AFM/STM modes
- Hybrid Mode™

- Modular high performance AFM/STM for wide range of applications
- Low noise and high resolution
- Full set of standard and advanced AFM/STM modes
- Hybrid Mode™

- SPM
- Automated AFM laser, probe and photodiode
- Confocal Raman / Fluorescence / Rayleigh Microscopy
- Tip Enhanced Raman Scattering (TERS)
- TERS optimized system for all possible excitation/detection geometries
- Hybrid Mode™

- IR sSNOM system
- High resolution AFM
- Stabilized CO₂ laser
- Hybrid Mode™

PIEZO SCANNING COORDINATES (CLOSED LOOP):

AFM integration with LIGHT

Mirror scanning (α, β)

OPTICAL DETECTION

- Confocal Raman/Fluorescence microscope
- Photon counting PMT, APD
- Lock-in detection ($\omega, 2\omega, 3\omega \dots$)
- Gated photon counting
- Time resolved (FLIM)
- Laser confocal microscopy

Tip, XYZ

AFM/STM/SNOM probe

laser spot

Sample, XYZ

Objective, Z

100x, 1.45 NA

Mirror scanning (α, β)

Mirror scanning (α, β)

NTEGRA Spectra II in Upright, Inverted and Side illumination configuration

Light input from side (with scanning mirror)

Top optics (LED illuminator & camera)

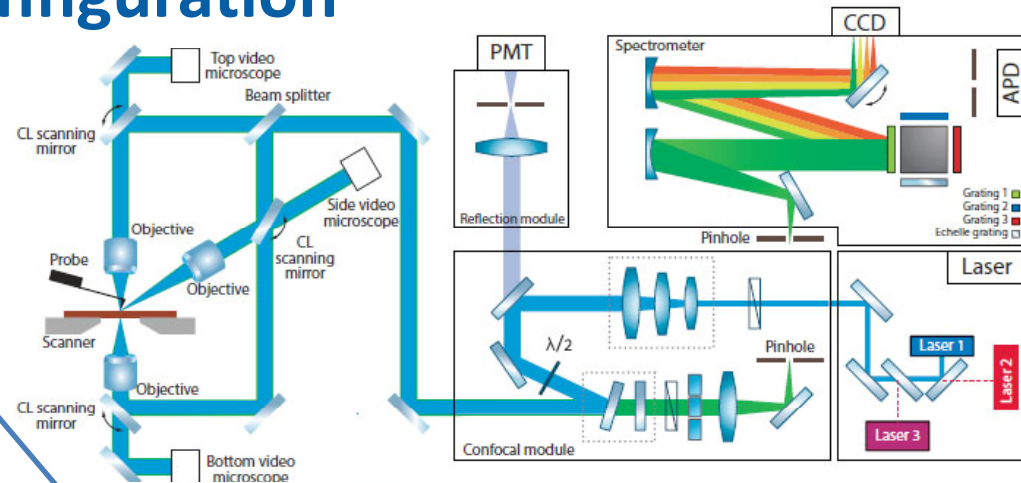
Light input from top (with scanning mirror)

Optical AFM (AFM probe + 100x objective on the top)

XYZ sample stage (bottom illumination objective inside)

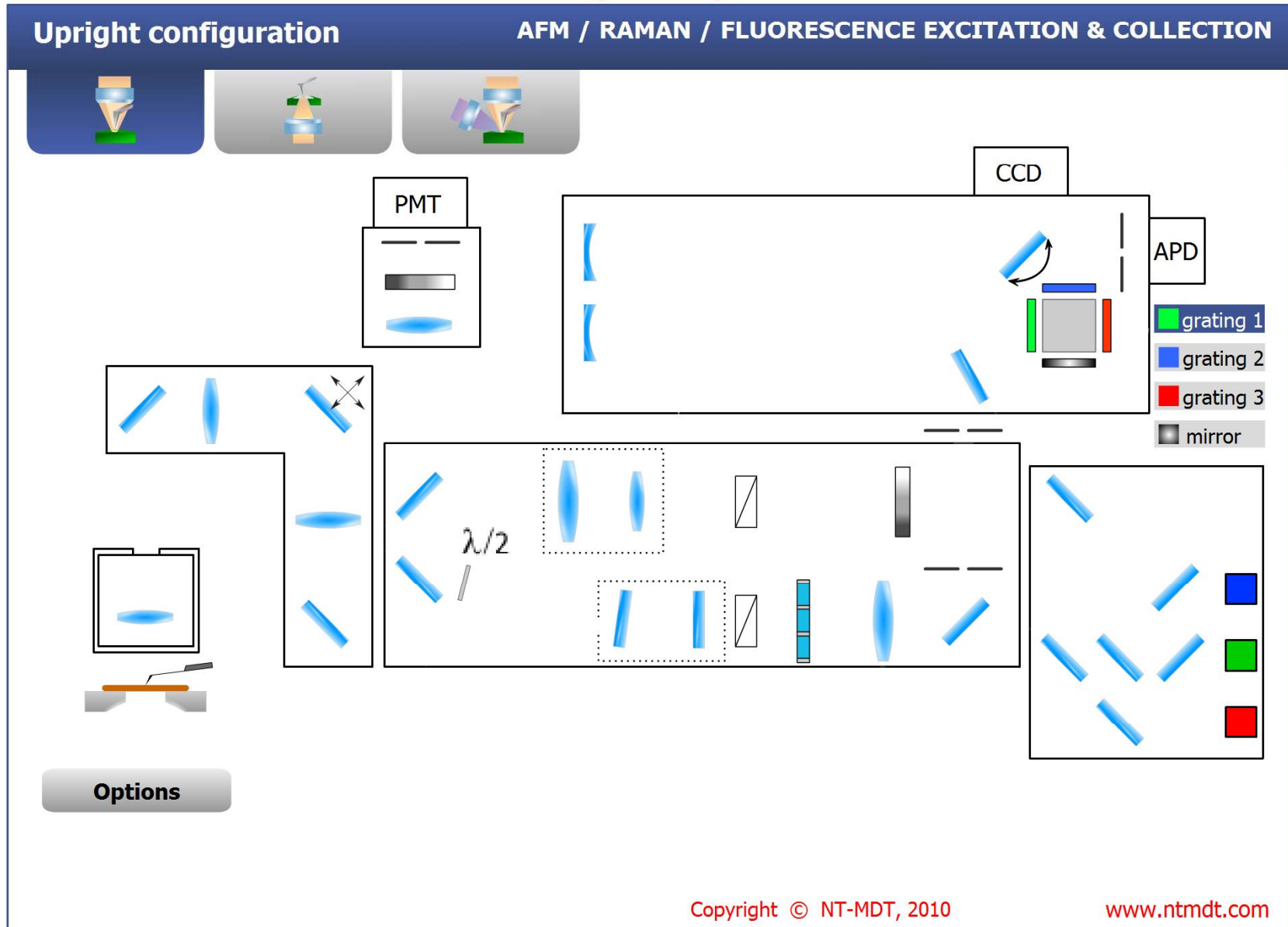
Light input from bottom (with scanning mirror)

Bottom optics (LED illuminator & camera)

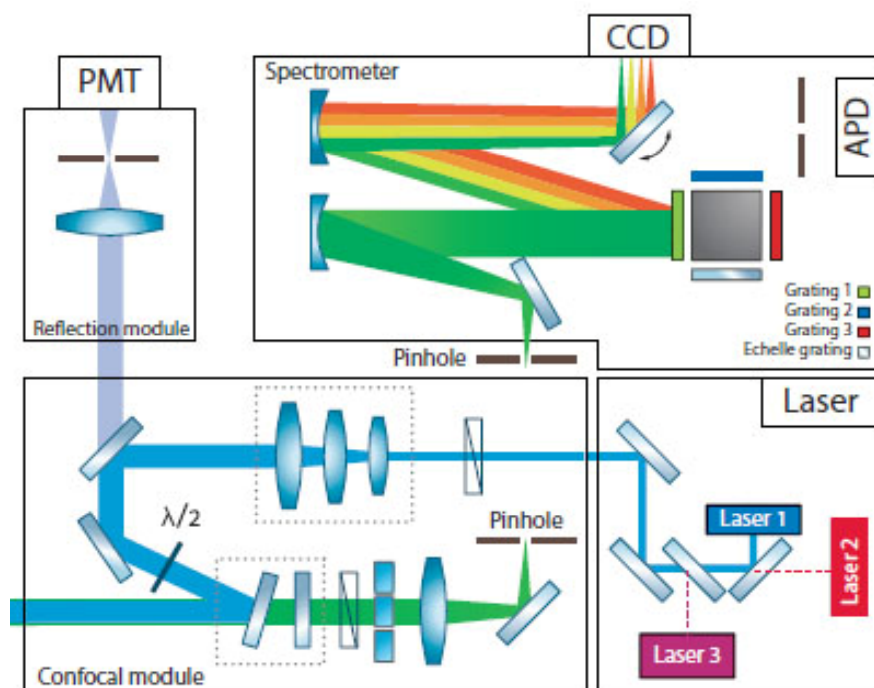


AFM – Confocal Raman / Fluorescence – SNOM – TERS

NTEGRA Spectra optical scheme

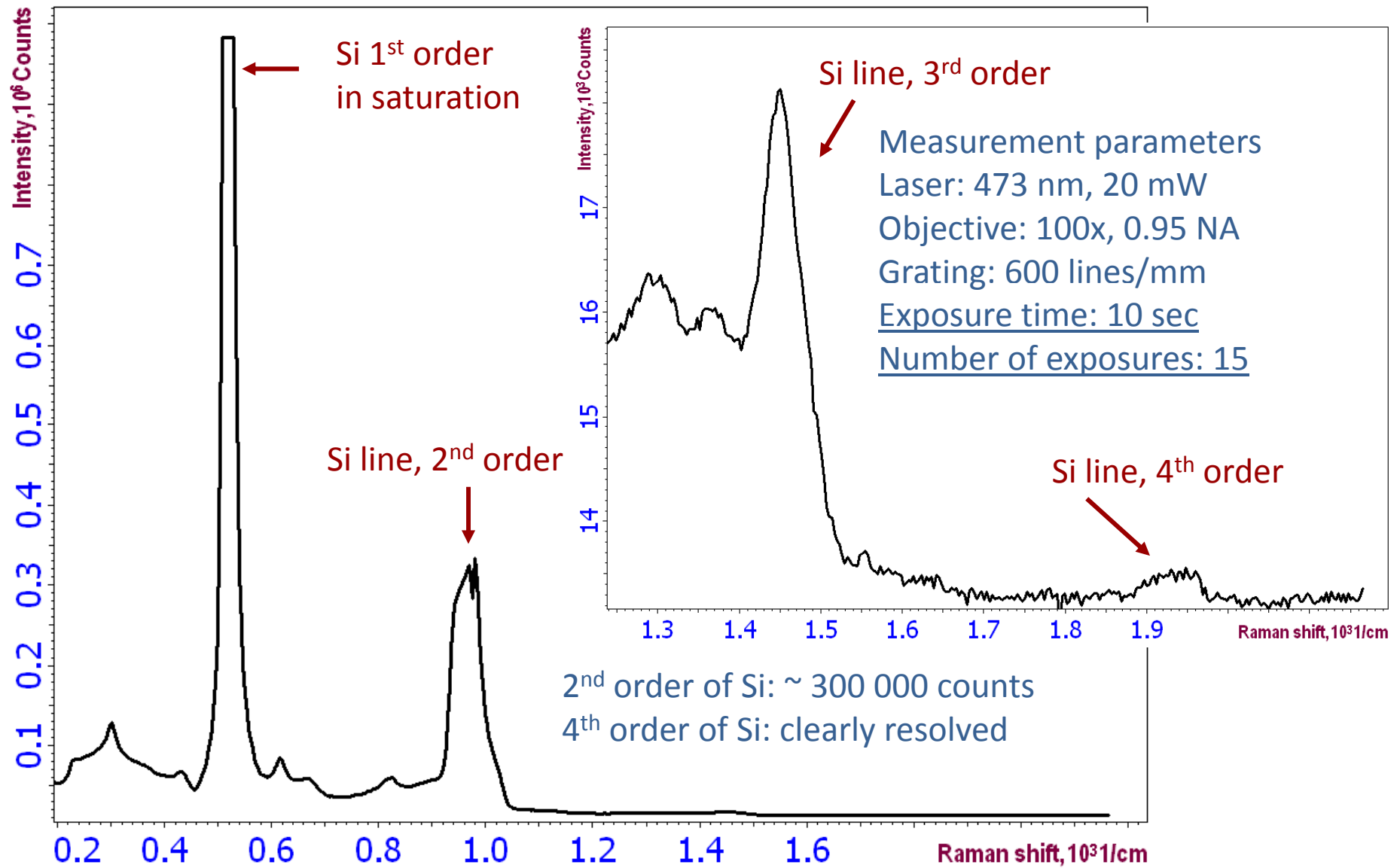


Optical scheme of Spectrometer

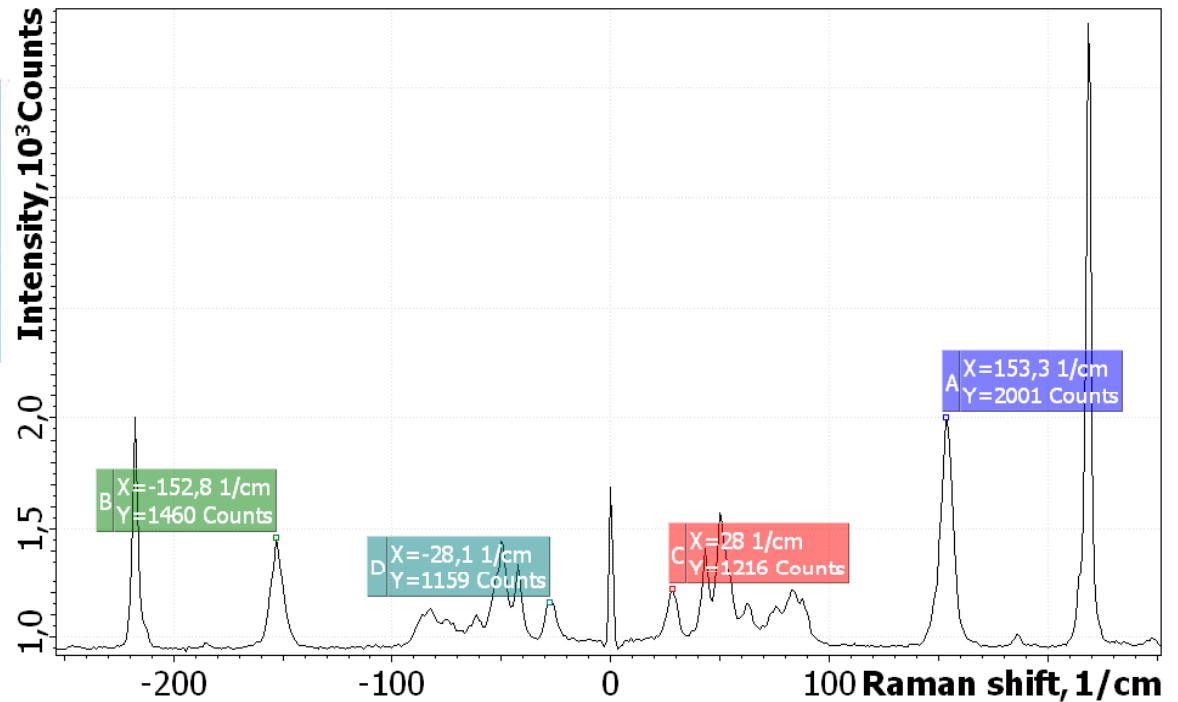
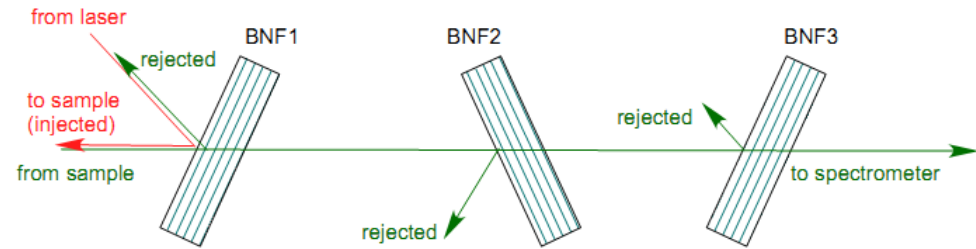
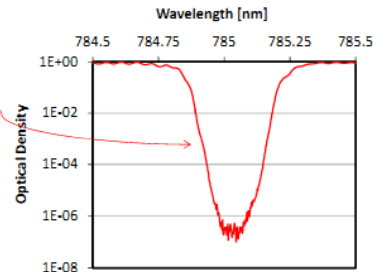
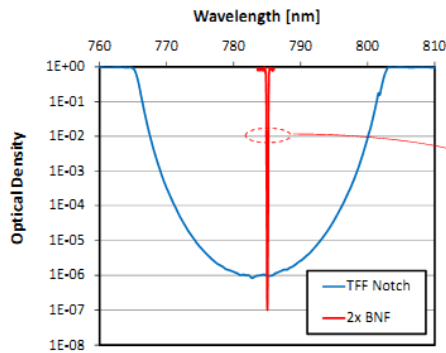


- True confocal design. Motorized confocal pinhole.
- Diffraction limited resolution guaranteed (e.g. 200 nm for blue laser, immersion optics)
- Extremely high optical throughput (~70-80 % for spectrometer, ~40-50% sample-to-detector)
 - Fully motorized laser change (up to 3 / 5 lasers). UV – VIS – IR region
 - Fully motorized: polarization optics, zoom beam expander, pinhole, 4 gratings
 - Can be equipped by fastest and most sensitive detectors available (FI/BI CCD, EMCCD, DD-CCD etc.)
 - Zoom beam expander – to guarantee diffraction limited laser spot to every objective
 - Three optical ports for detectors: two in monochromator, one in separate channel

Sensitivity: 4th order of Si Raman band is clearly resolved



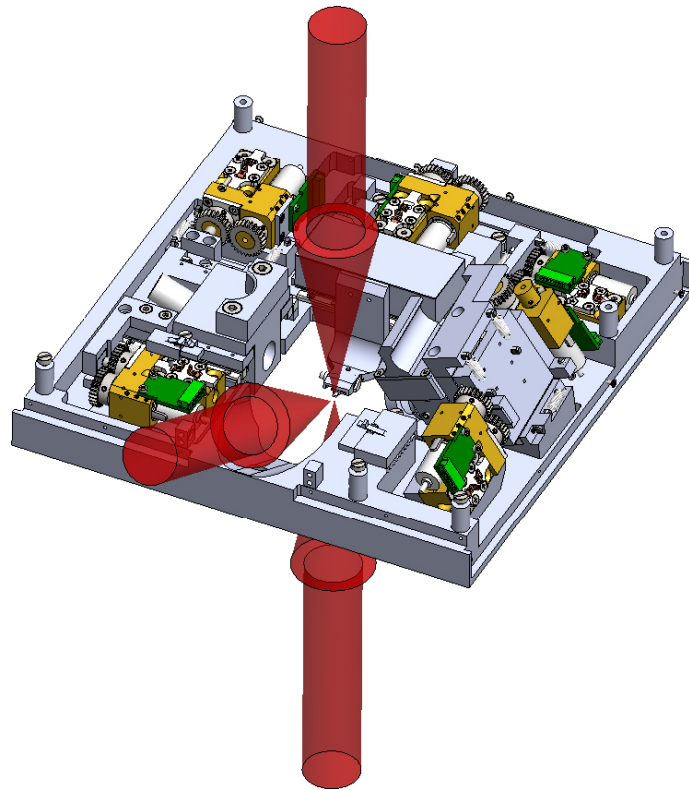
Low wavenumbers Raman spectra



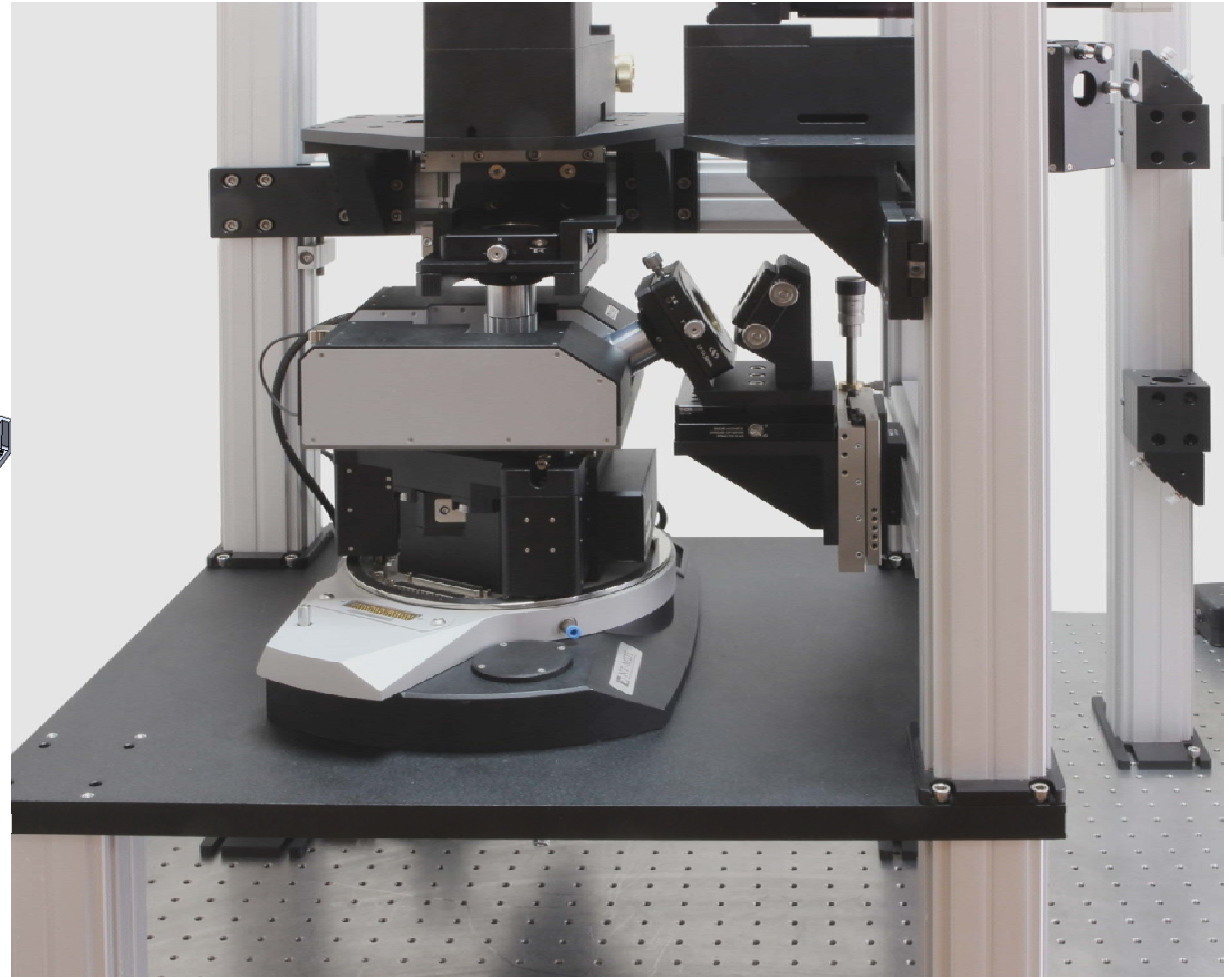
Low wavenumbers Raman spectrum of sulfur. Cut-off at 10 $1/cm$
488 nm laser, 1800 lines/mm grating.

Optical access from Top, Bottom and Side

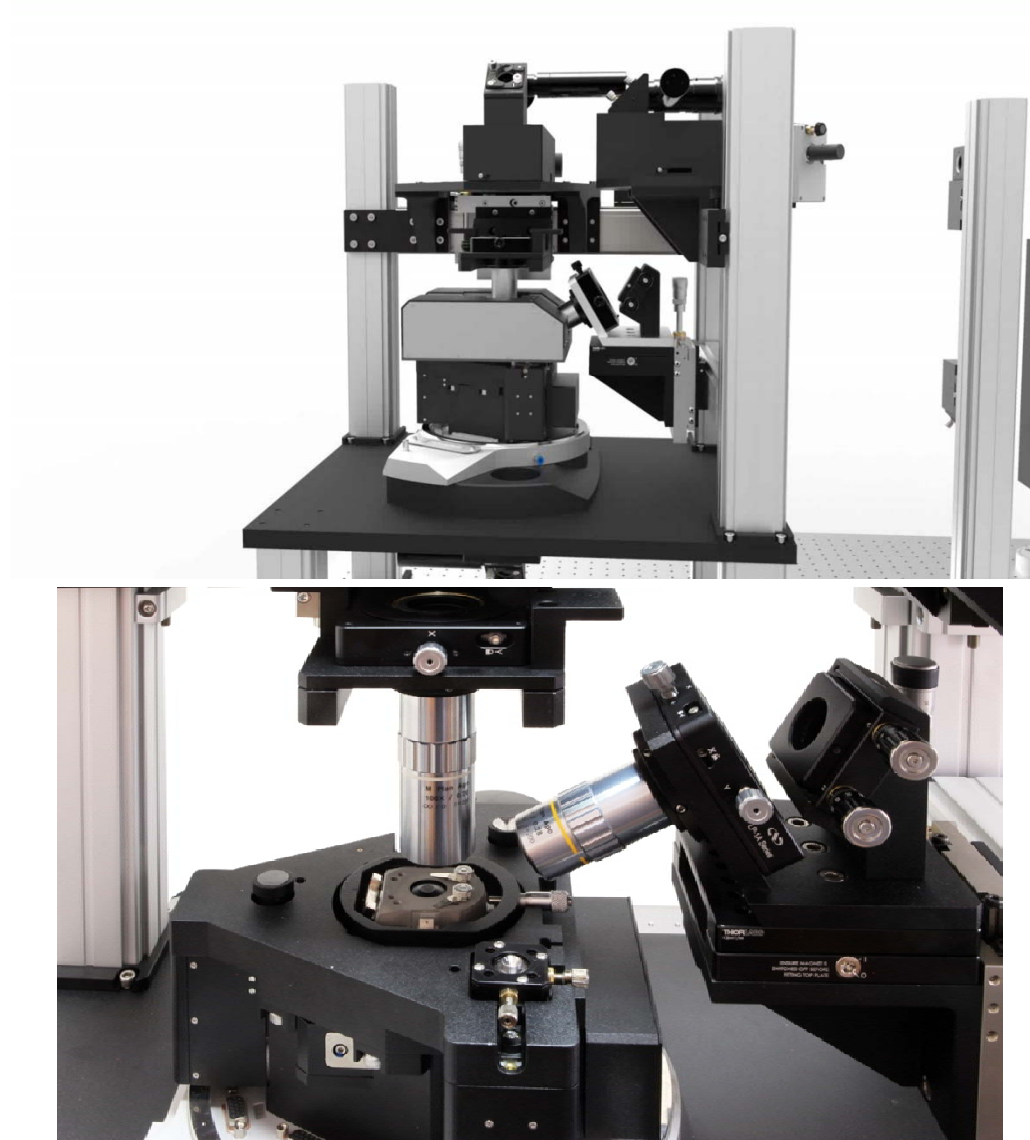
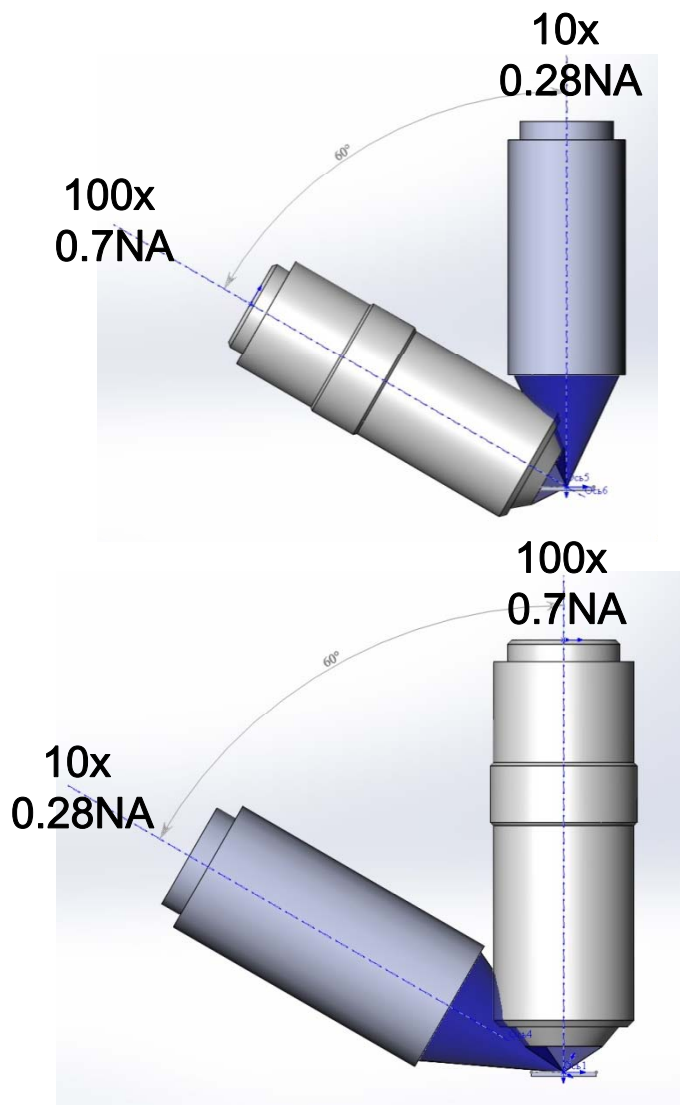
Access for **Mitutoyo** long working distance objective for top illumination



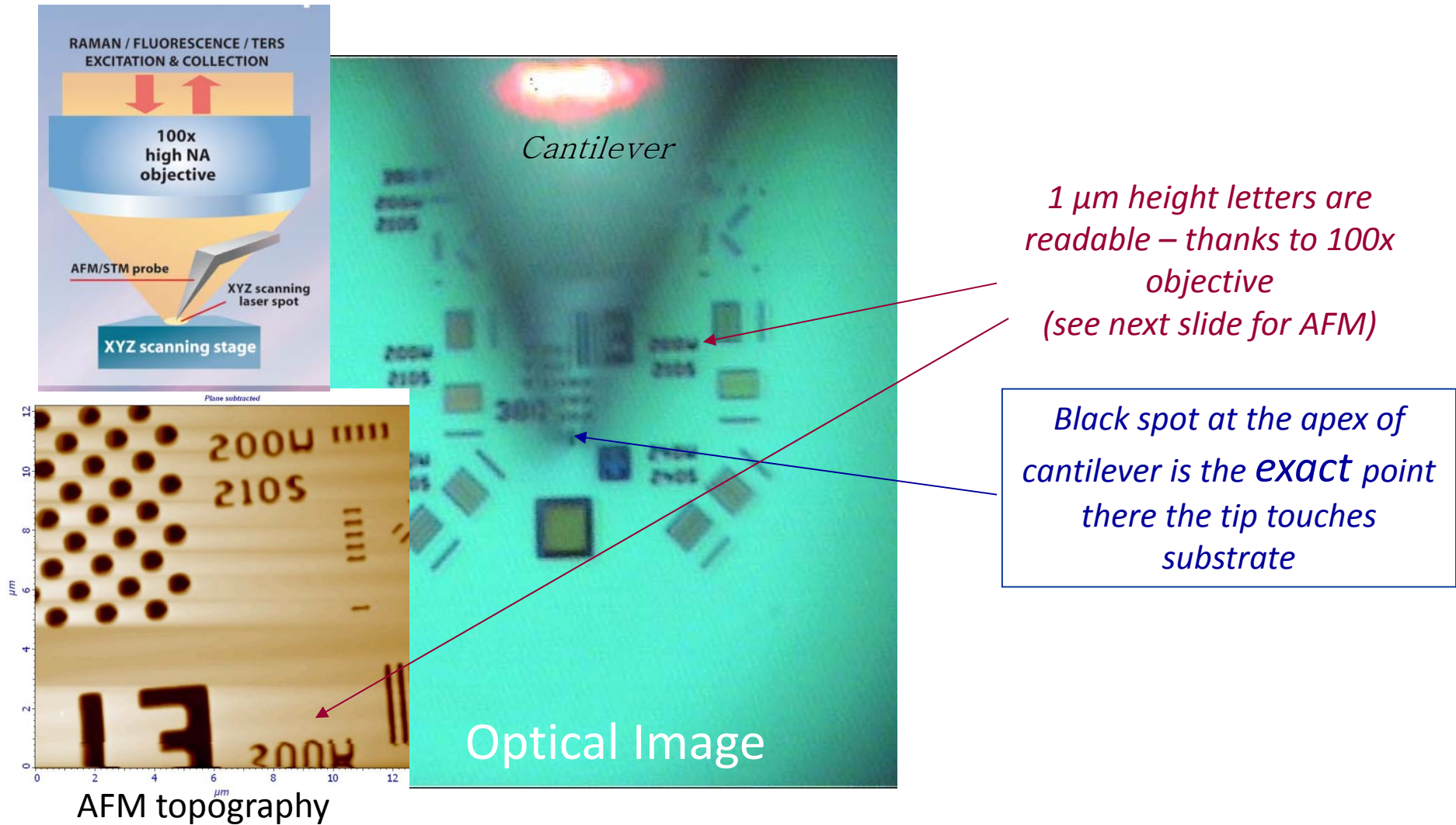
Access for bottom illumination objective



Excitation-collection configurations



Top optical access to the AFM probe with 100x objective

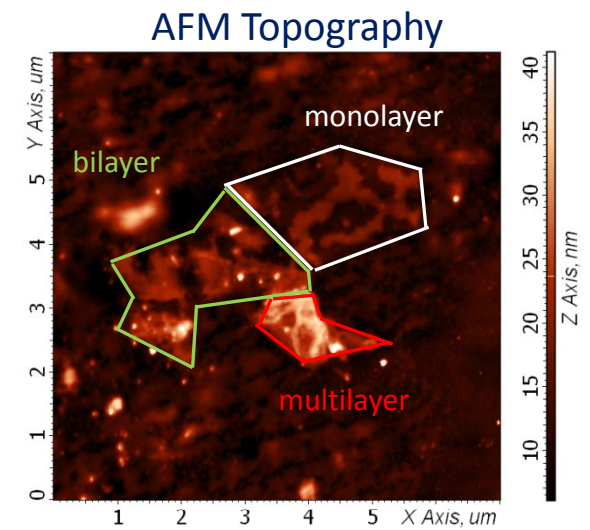
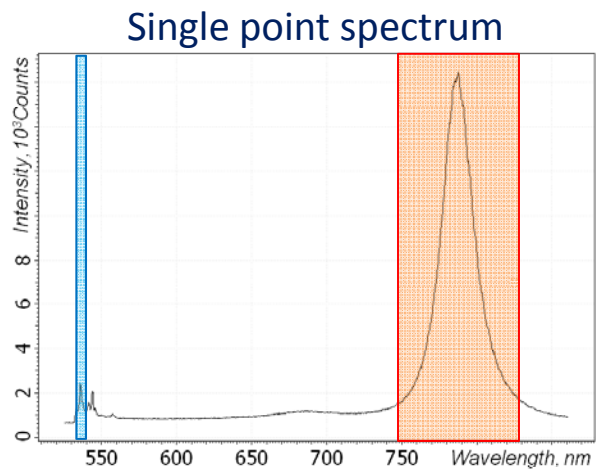
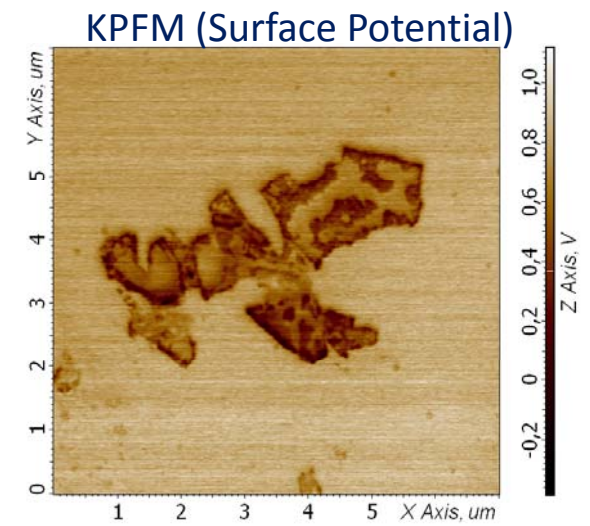
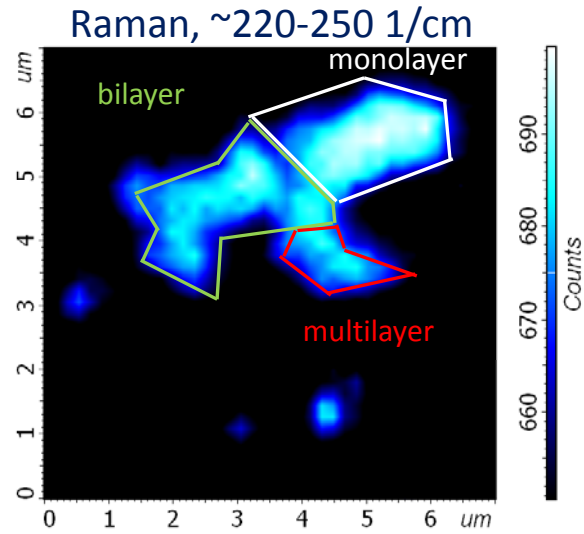
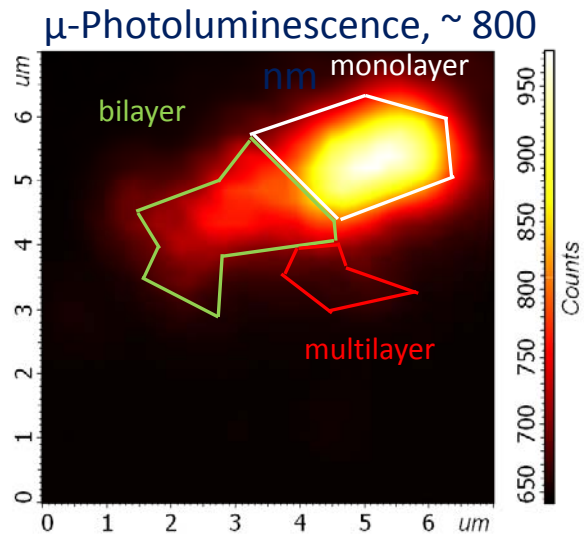


AFM probe over a structured Si substrate. View through 0.7NA 100x objective

Apex of opaque Si tip looks transparent on the image!

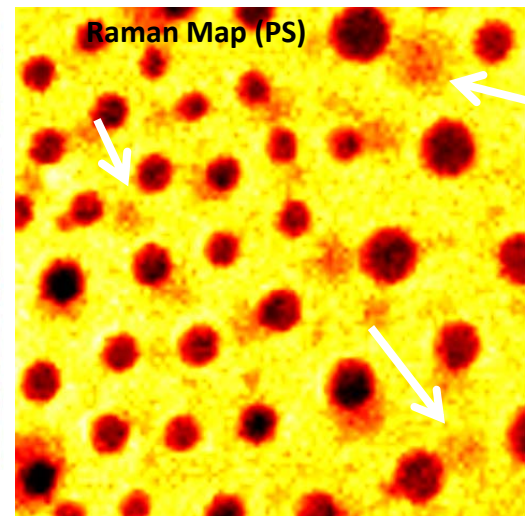
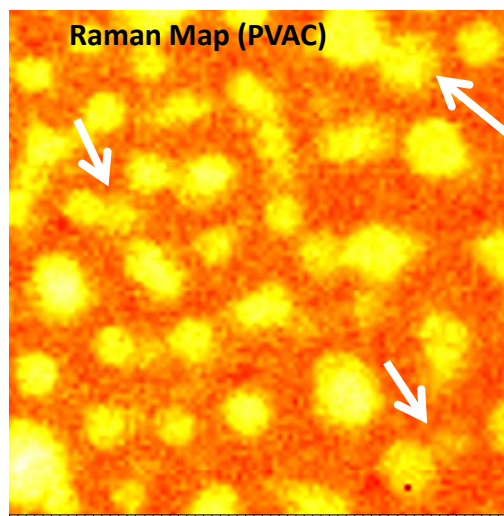
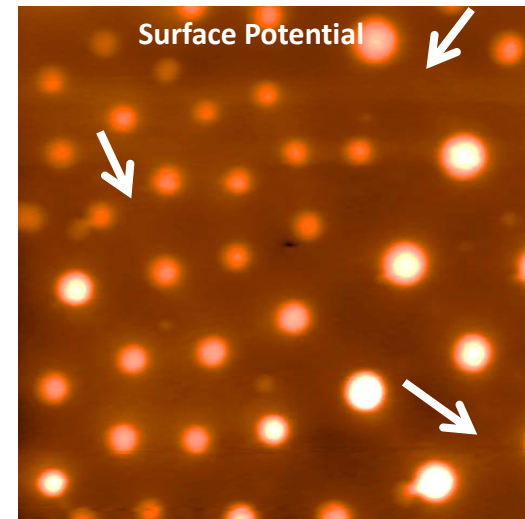
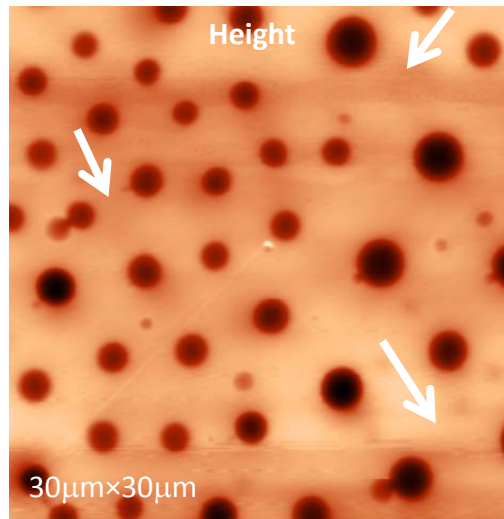
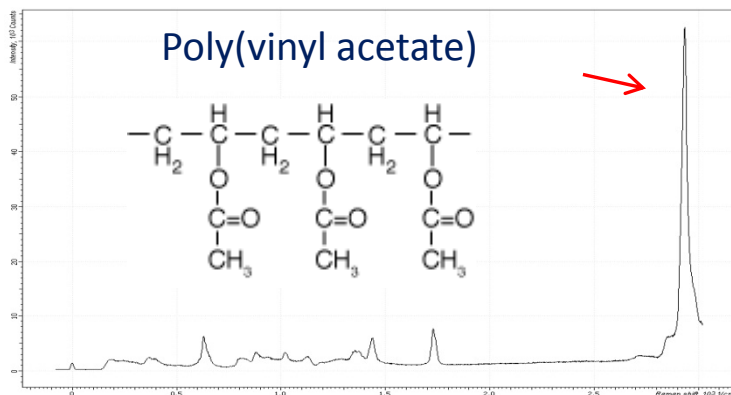
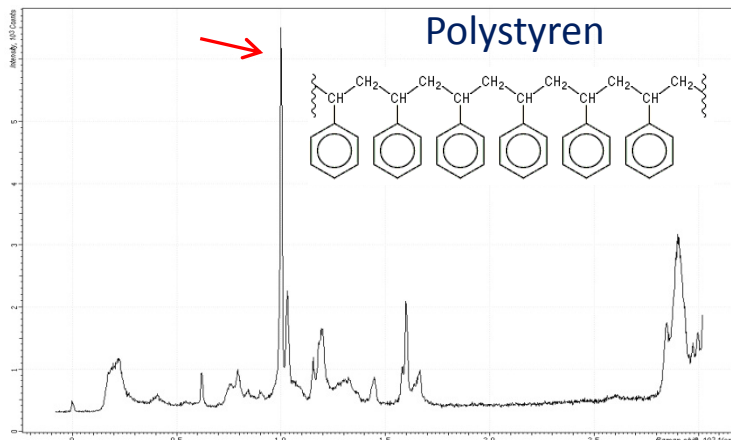
This unique observation is due to high aperture (0.7 NA) of the imaging objective

MoSe₂ flakes

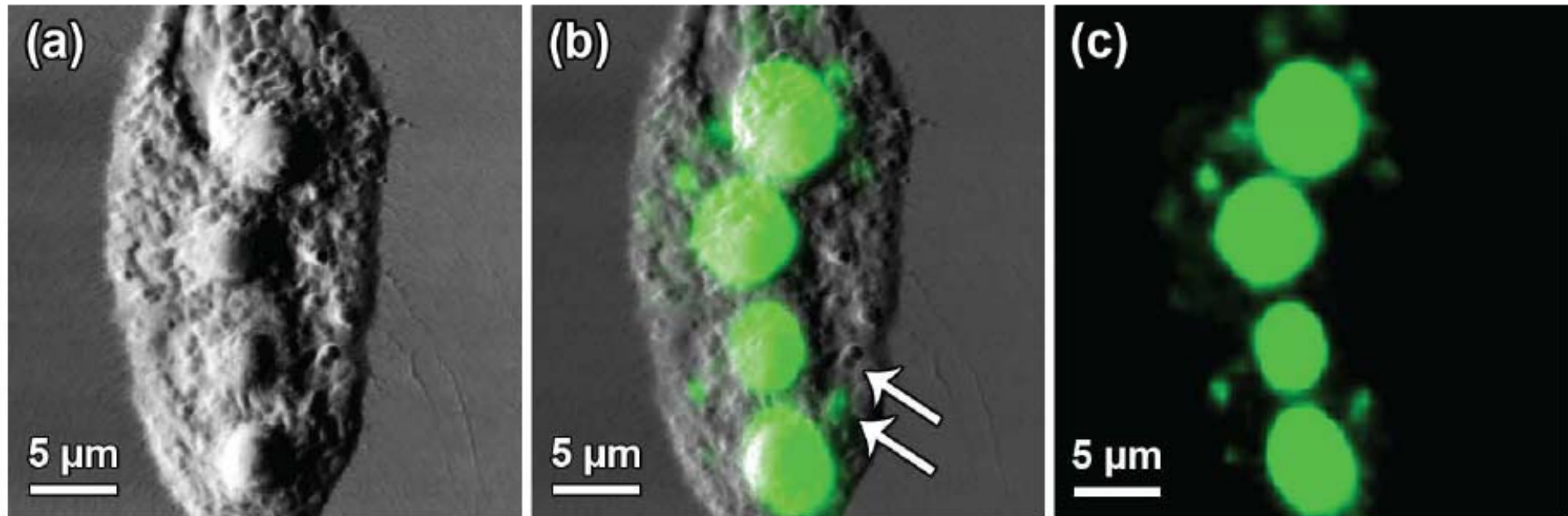


KPFM-Raman Studies of Polymer Blends

Polymer Blend PS-PVAC: Thick Film on ITO glass



Cyanobacteria biofilm: AFM and Raman mapping

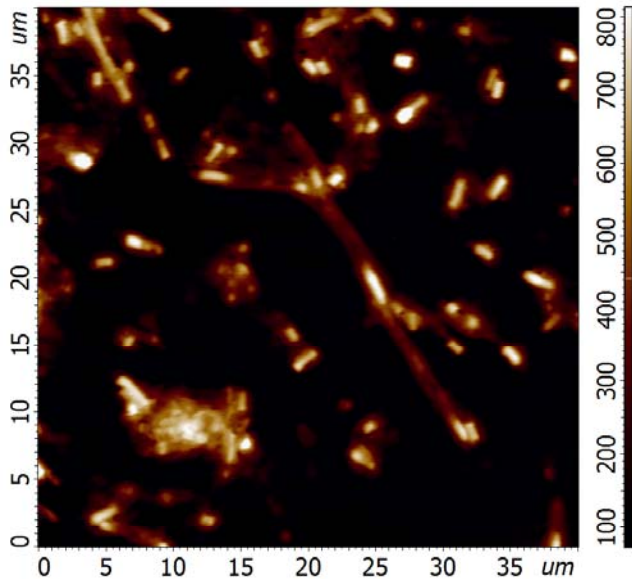


Combined study of cyanobacteria biofilm by means of atomic force microscopy and confocal Raman microscopy. AFM image in phase contrast (left) gives an image with nm resolution, however, does not contain any chemical information. Raman map (right) corresponds to the distribution of beta-carotene. Resolution Raman map is limited by the optical limit and is 400-500 nm. Beta-carotene is the pigment contained in cyanobacteria which perform photosynthesis. Overlay of two images (center) provides the chemical identity and relate it to the AFM image of high resolution.

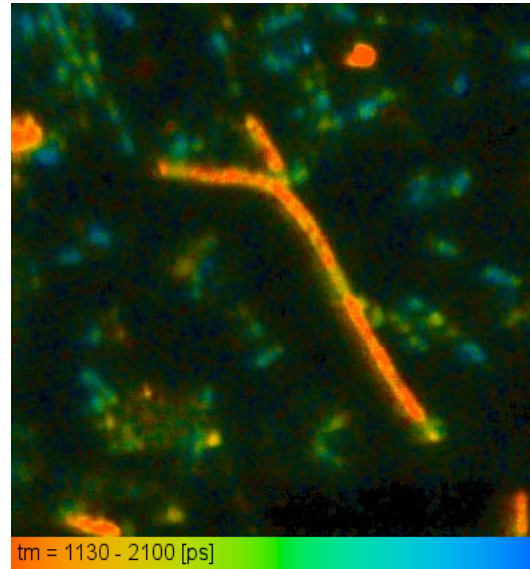
Data courtesy: Thomas Schmid, Pawel L. Urban, Andrea Amantonico, Renato Zenobi ETH Zurich, Switzerland

Topography and FLIM image of e-coli

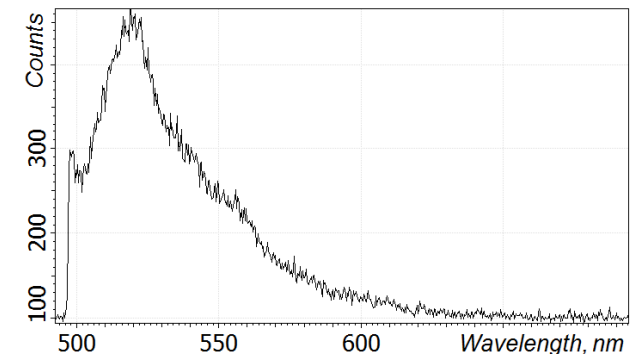
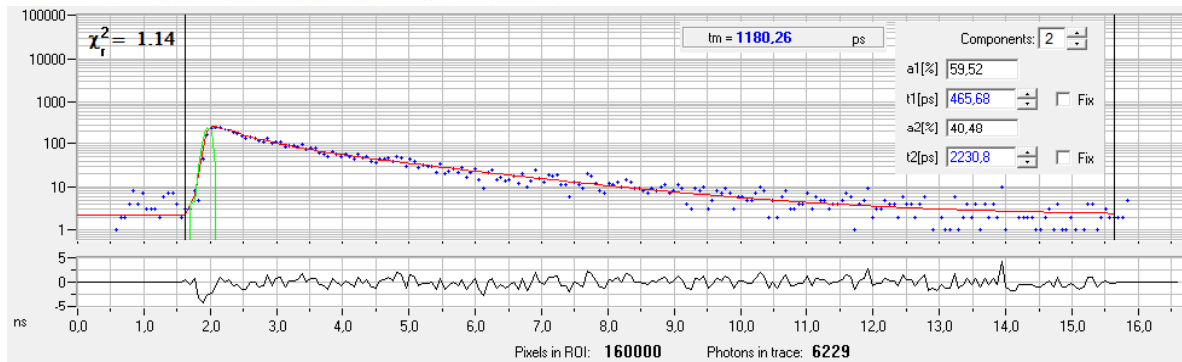
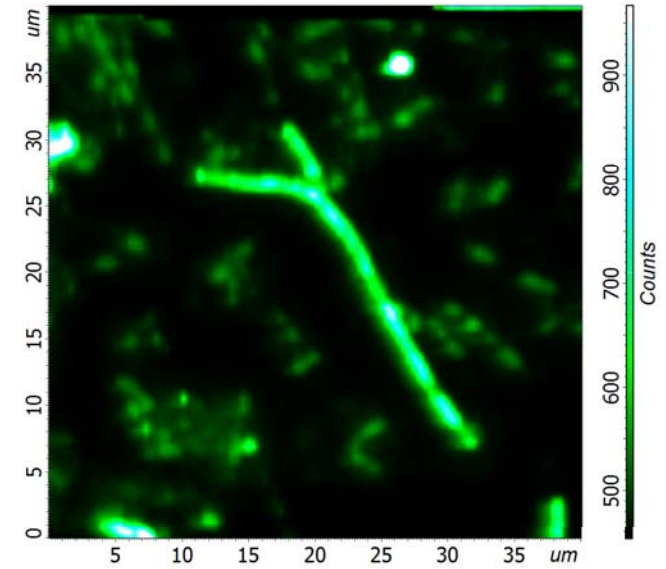
AFM Topography



Lifetime map 525-540 nm

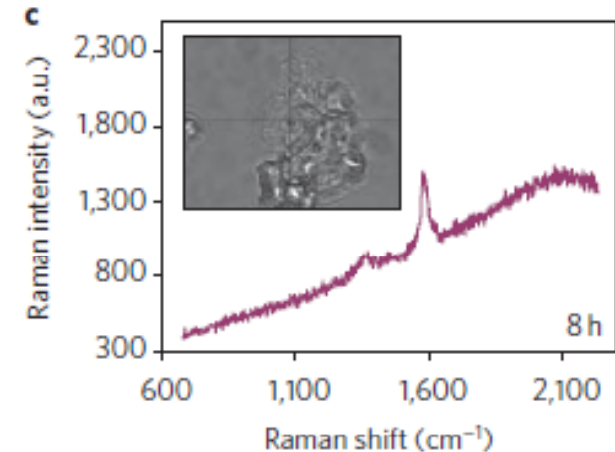
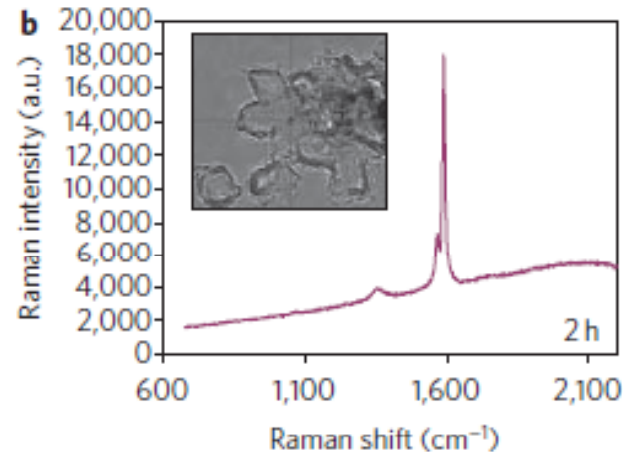
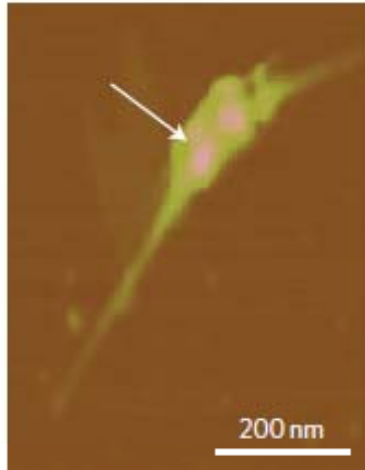


Fluorescence 525-540 nm



Topography (left) and FLIM mapping of 525-540 nm band (center) and fluorescence intensity (right). Decay curve on the bottom left image and fluorescence spectrum on the bottom right one. Different FLIM signals come from different fluorescent proteins, which produced by e-coli genetically modified in different ways. Spectrum shape is very similar. Intensity and lifetime is different. AFM + Spectrometer + FLIM provides sufficient information to identify different proteins in bacteria.

Biodegradation of carbon nanotubes

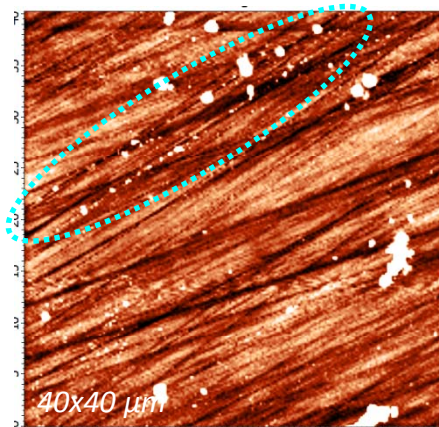


AFM image showing the capture of a single nanotube by living cell of immune system (neutrophils).

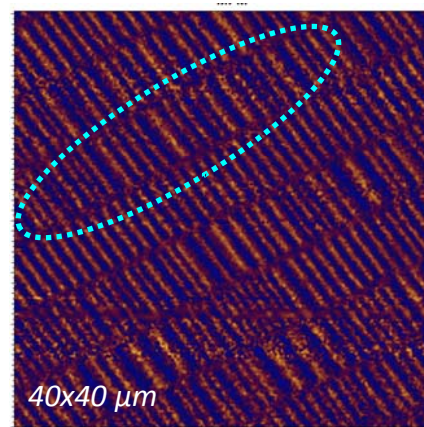
Raman spectra of neutrophil with IgG-nanotubes after 2 hours (b) and 8 hours (c). Reducing the intensity of G- and D-bands of carbon nanotube indicates biological degradation of single nanotubes. Thus, neutrophils were successfully processed and excreted objects such as carbon nanotubes

Y. Volkov et al // Carbon nanotubes degraded by neutrophil myeloperoxidase induce less pulmonary inflammation, Nature Nanotechnology, 2010

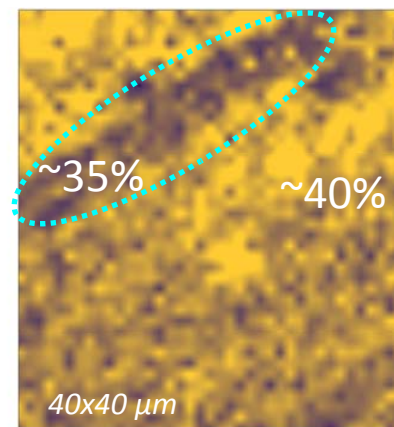
DLC Protective Layer of Hard Disk Drive



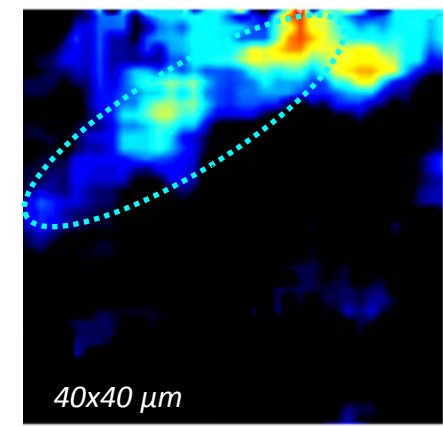
AFM topography
Nearly parallel scratches in
DLC protective layer are
produced by low-flying
magnetic head. Bumps are
signatures of erosion of Co
magnetic layer.



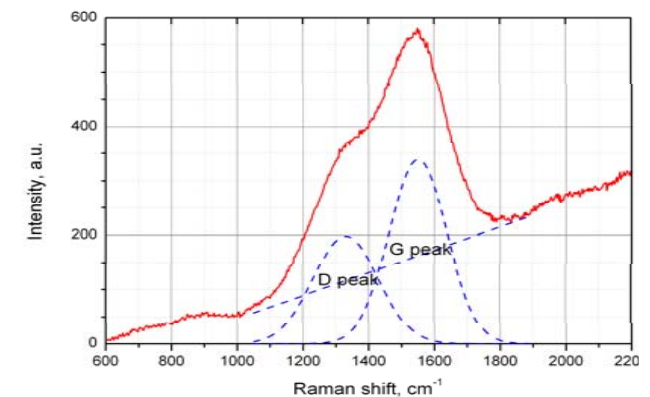
MFM image
Magnetic domains
are not damaged yet.



Raman map,
sp3 (diamond-type)
bonding fraction
 $\omega_G = 1580$.

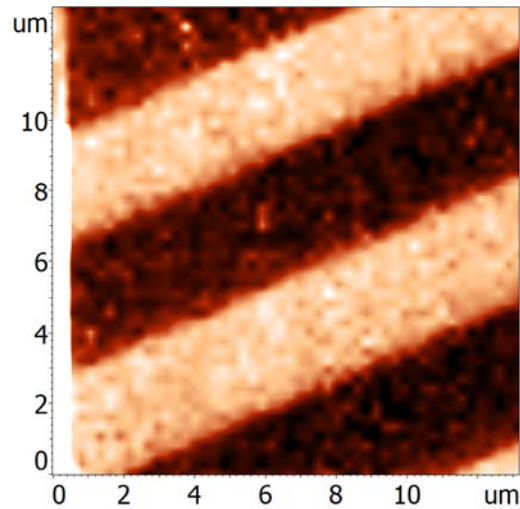


Raman map,
ID/IG ratio
Increased fraction of
sp2 bonds and
defects.

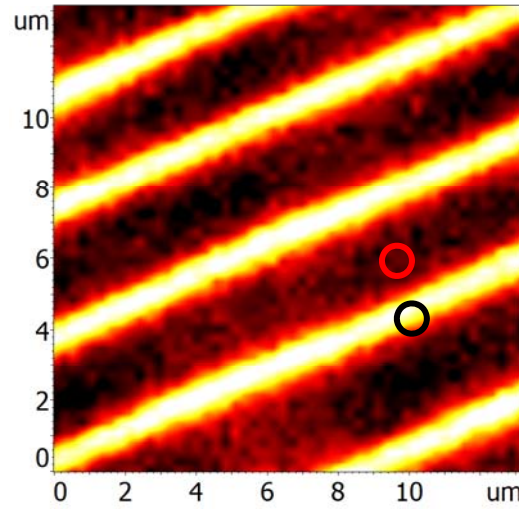


Simultaneous PFM and Raman mapping

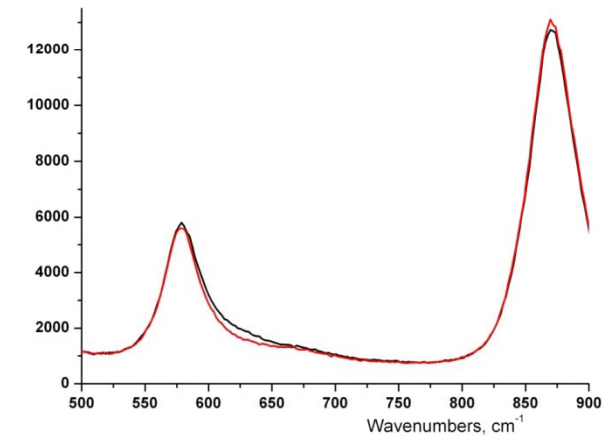
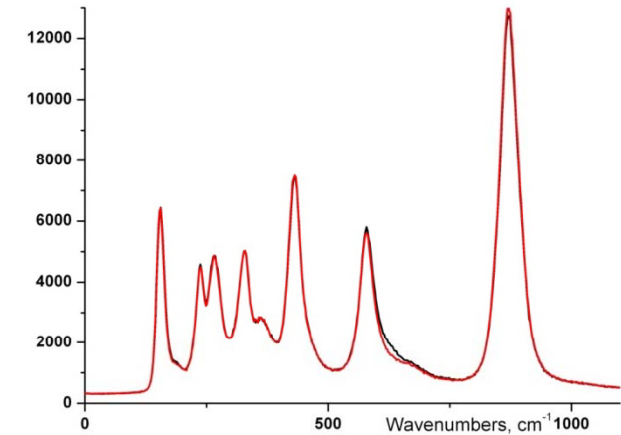
PFM



Raman map of band
553-599 1/cm

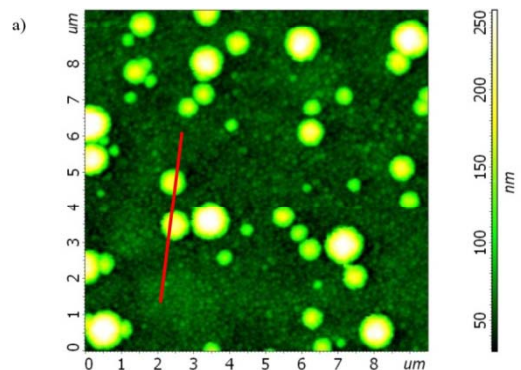


PFM mapping and Raman mapping of 553-599 1/cm band Lithium Niobate. Changes of Raman bands intensities appears on the border of domains

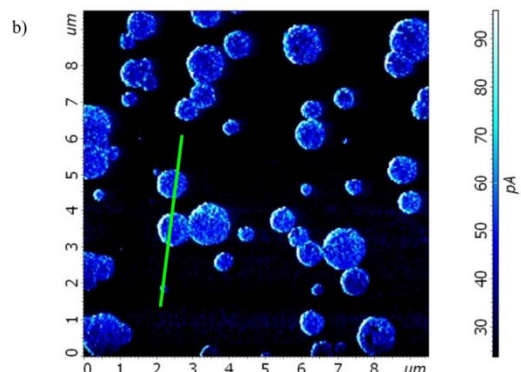


100x0,7 objective used. ~8 mW of 473 nm laser used.
Exposure time 1 s/points and 50x50 points scan size.

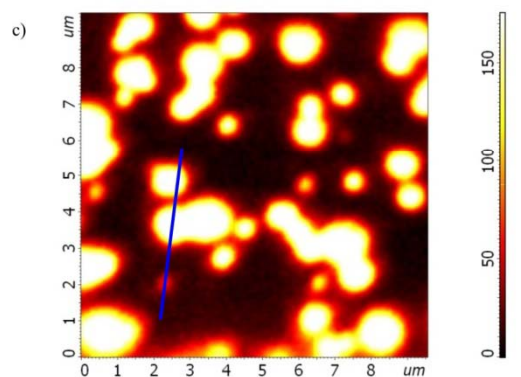
Photocurrent mapping under localized optical excitation



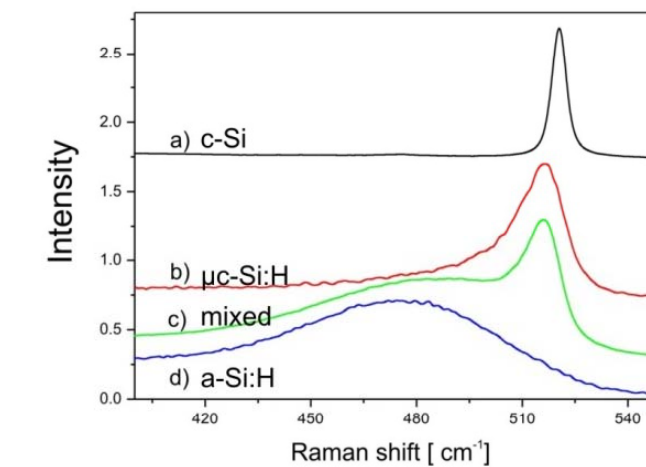
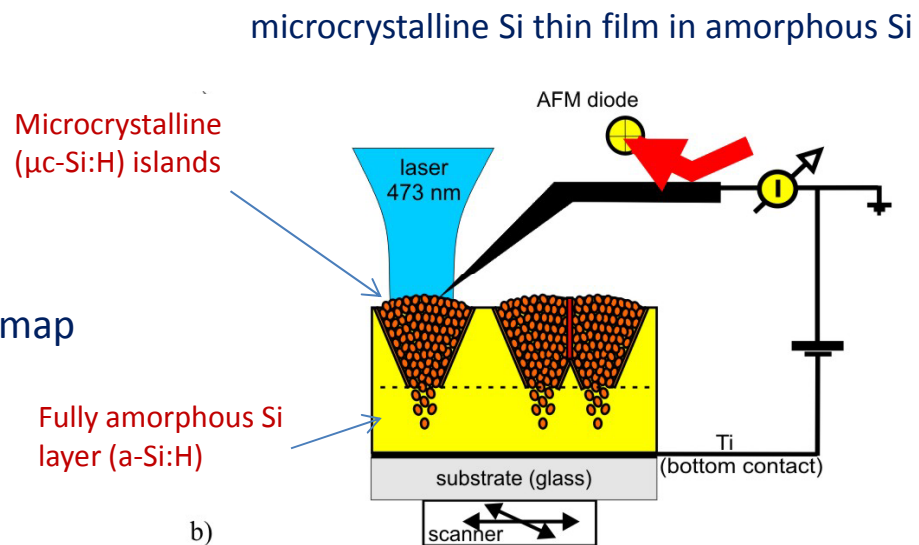
Topography map



Local photoconductivity map



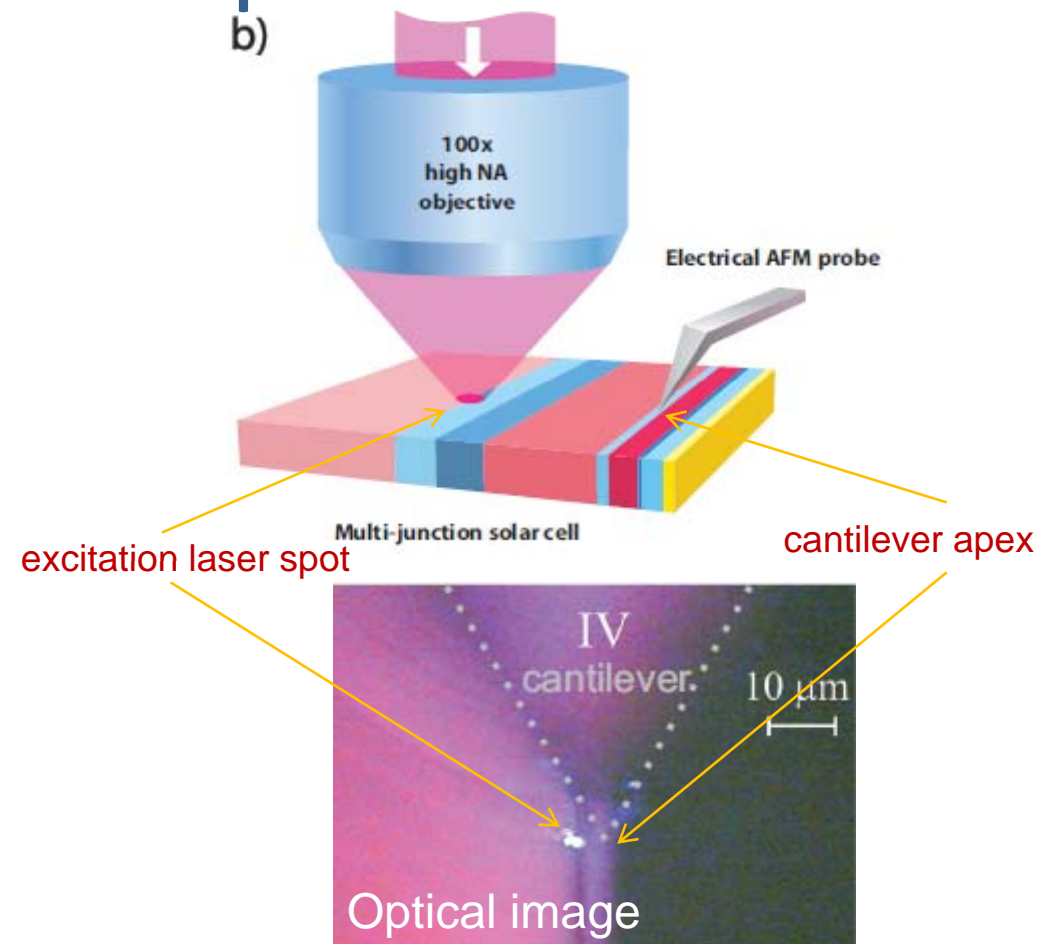
Raman map ($\mu\text{c-Si:H}$)



Solar cell diagnostics by combination of Kelvin probe microscopy with local photoexcitation

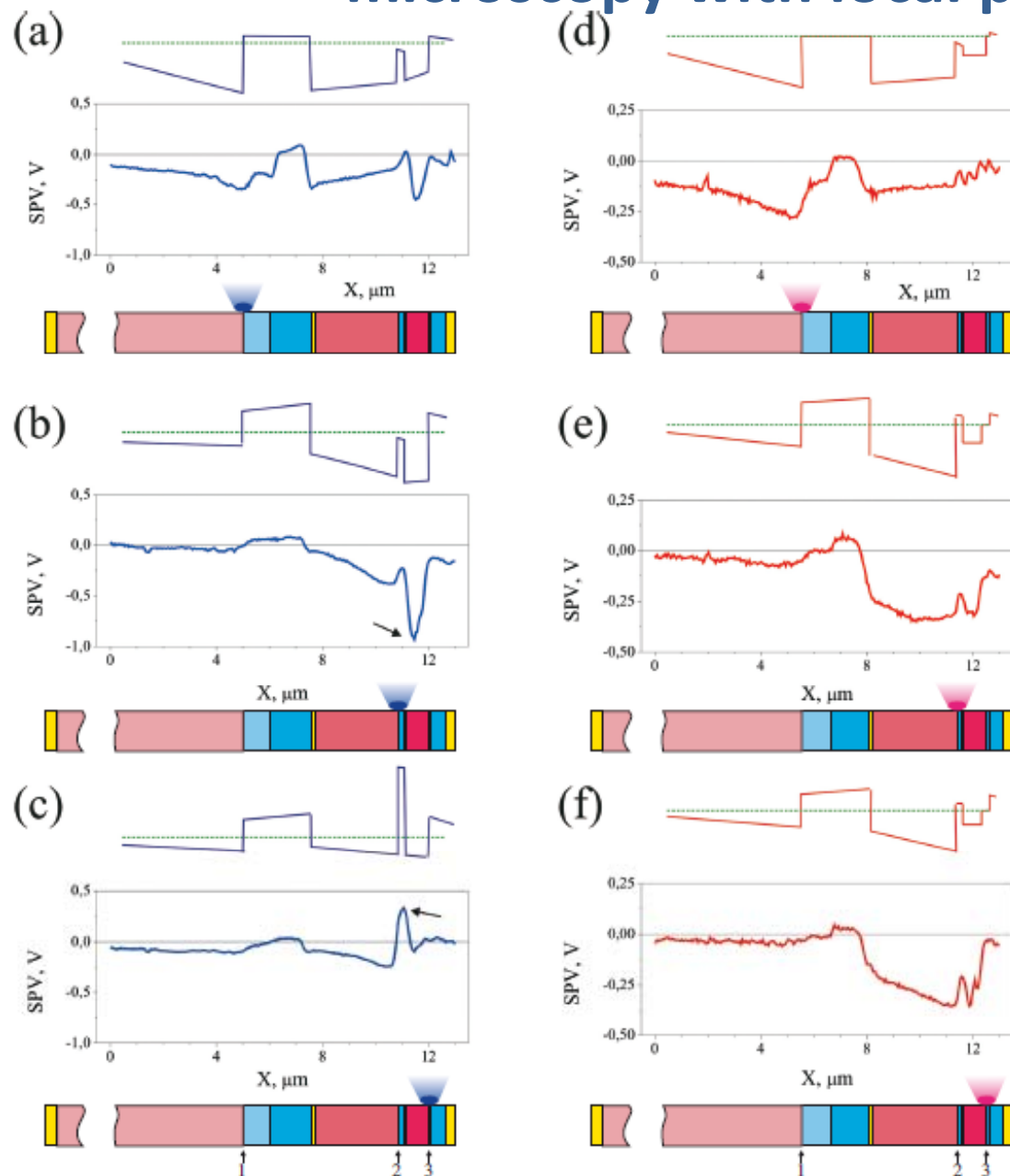
	Ga _{0.99} In _{0.01} As-n ⁻	500 nm
	Al _{0.51} In _{0.49} P-n	30 nm
3→	Ga _{0.51} In _{0.49} P-n	50 nm
	Ga _{0.51} In _{0.49} P-p	680 nm
	Al _{0.25} Ga _{0.25} In _{0.5} P-p	50 nm
	Al _{0.4} Ga _{0.6} As-p ⁺⁺	15 nm
	GaAs-n ⁺⁺	15 nm
	Al _{0.51} In _{0.49} P-n	30 nm
	Ga _{0.51} In _{0.49} P-n	100 nm
2→	Ga _{0.99} In _{0.01} As-n	100 nm
	Ga _{0.99} In _{0.01} As-p	~ 2500 nm
	Ga _{0.51} In _{0.49} P-p	100 nm
	Al _{0.25} Ga _{0.25} In _{0.5} P-p	30 nm
	Al _{0.4} Ga _{0.6} As-p ⁺⁺	30 nm
	GaAs-n ⁺⁺	30 nm
	Al _{0.53} In _{0.47} P-n	50 nm
	Ga _{0.99} In _{0.01} As-n	1000 nm
	Ga _{0.51} In _{0.47} P-n	100 nm
1→	Ge-substrate (n doped)	~ 300 nm
	Ge-substrate (p doped)	

Multijunction solar cell structure.
 Digits 1,2,3 show p-n junctions.
 Blue: n-type layers, pink: p-type layers,
 yellow: highly conductive layers



Individual p-n junction is locally excited by a 400 nm laser spot. Variation of surface potential is measured by cantilever (Kelvin probe microscopy)

Solar cell diagnostics by combination of Kelvin probe microscopy with local photoexcitation



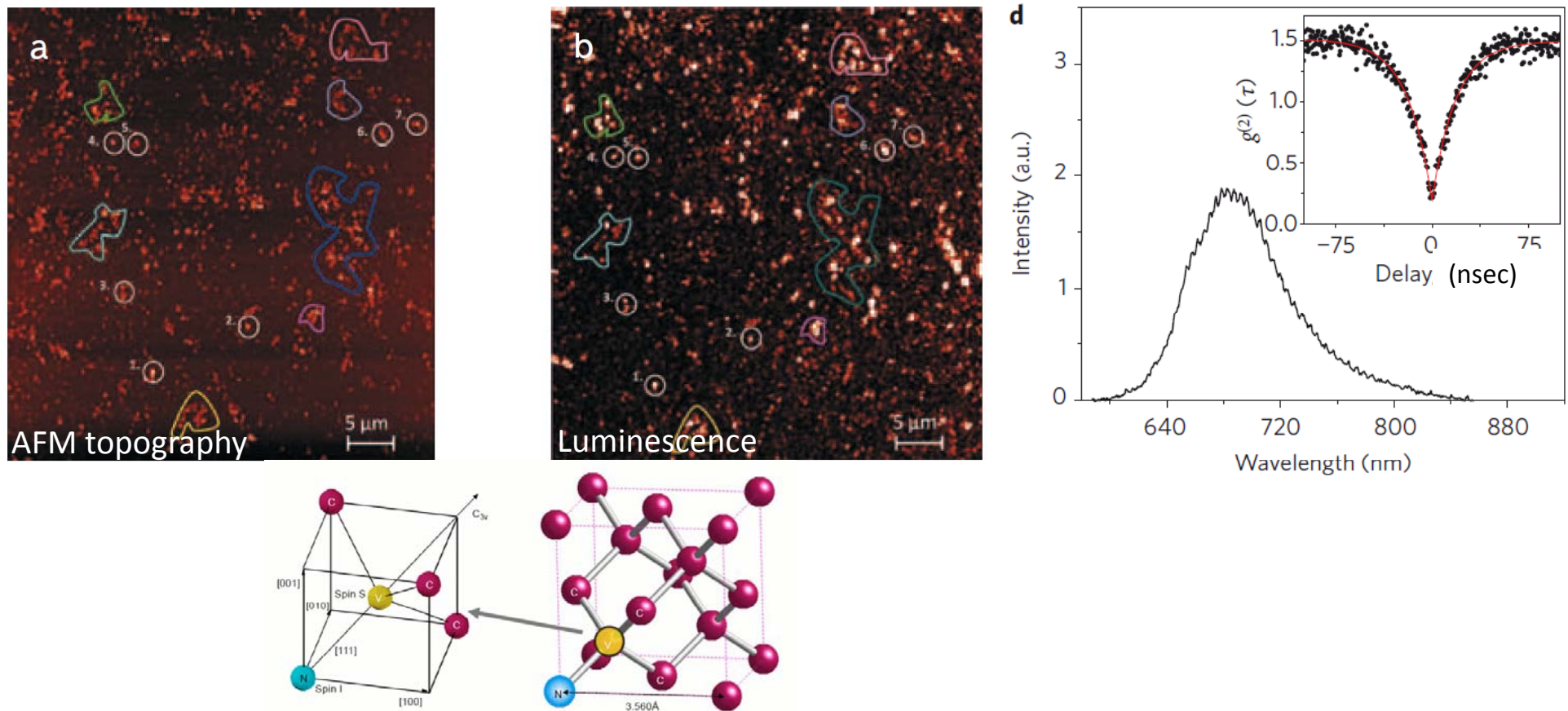
Surface potential variation for local excitation by 473 nm laser (left row: a,b,c) and 785 nm laser (right row: d,e,f).

Different individual p-n junctions are locally excited.

Experimental results correspond well to numerical simulation

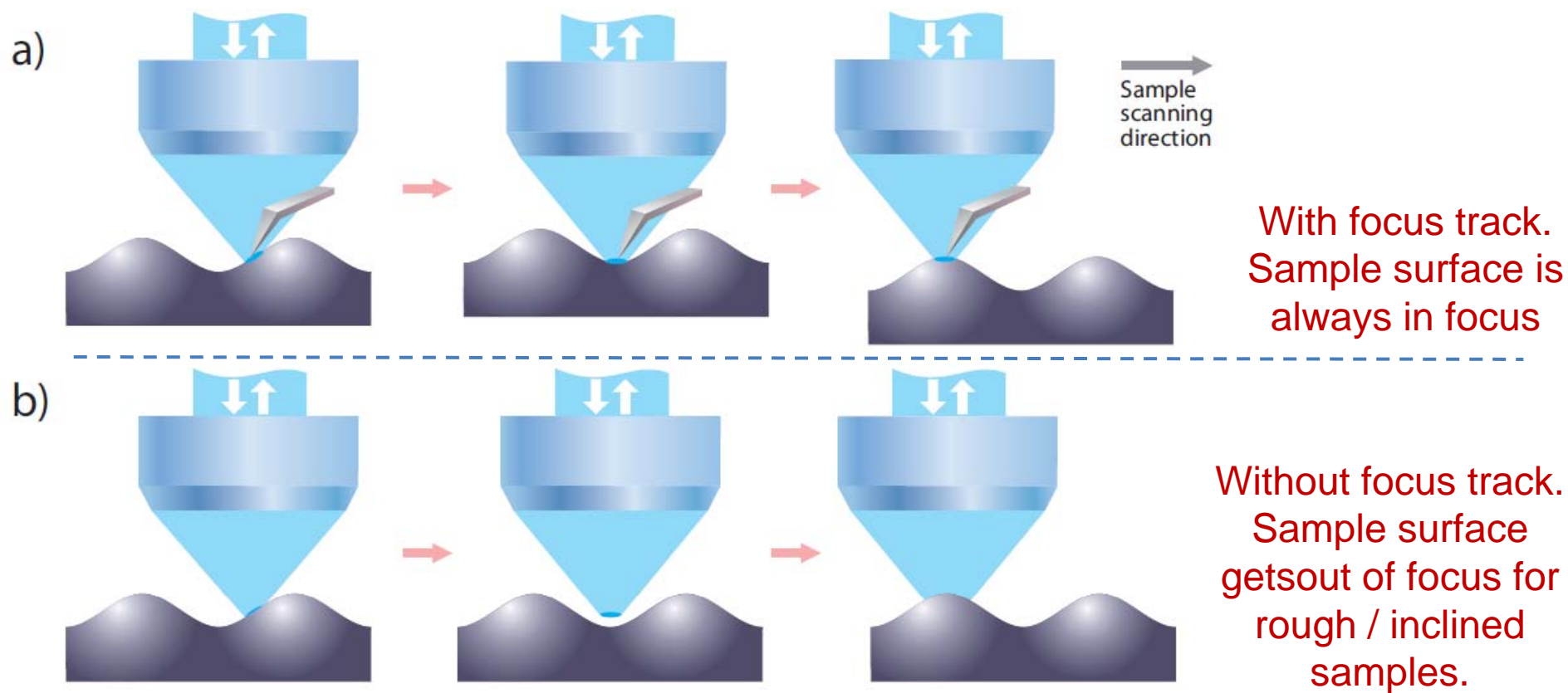
A. Ankoudinov, A. Shelaev Ioffe
Institute & NT-MDT

Nitrogen vacancy color centers in nanodiamonds



Observation of nitrogen-vacancy (NV) color centers in *discrete* detonation nanodiamonds
(a) AFM topography image; smallest particles observed are discrete isolated nanodiamonds of ~5 nm size. (b) Confocal luminescence map of the same sample area; nitrogen-vacancy luminescence from isolated nanodiamonds is clearly seen. (c) Luminescence spectrum of individual NV center in a 5 nm crystal host.

Focus track feature of integrated AFM - confocal Raman/fluorescence instrument

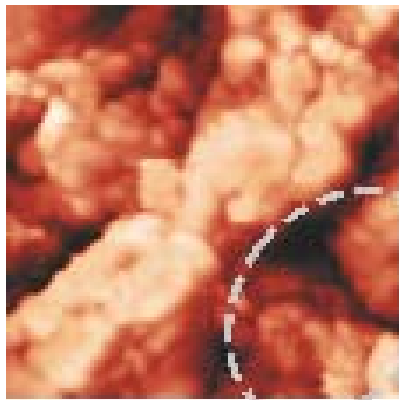
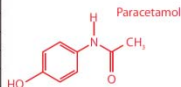
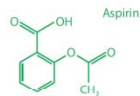
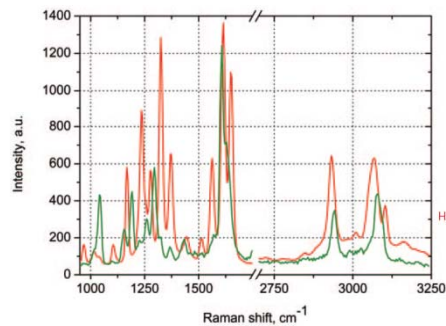


(a) Integrated AFM-Raman instrument and its “focus track” feature. Sample surface always stays in focus due to AFM feedback mechanism. This provides true information about sample chemical composition even for very rough surfaces.

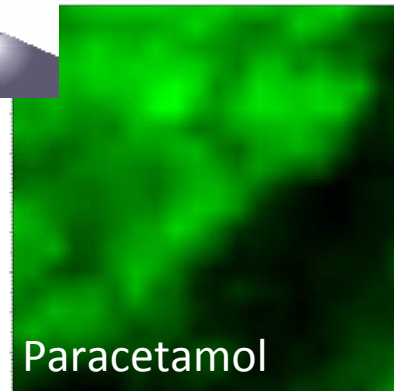
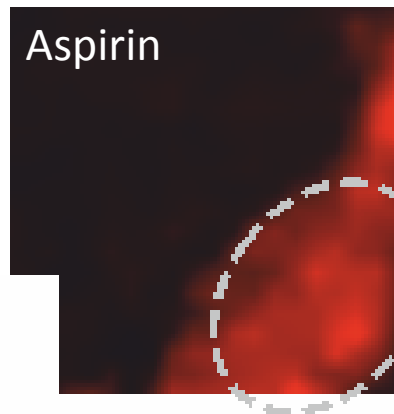
(b) Standard confocal Raman/fluorescence imaging – sample is scanned in X&Y directions; Sample gets out of focus, providing incorrect data about optical properties of the surface.

Focus track feature of integrated AFM - confocal Raman/fluorescence instrument

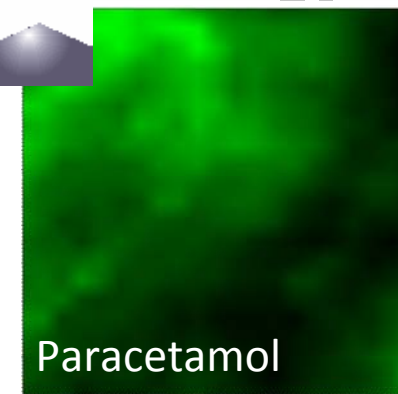
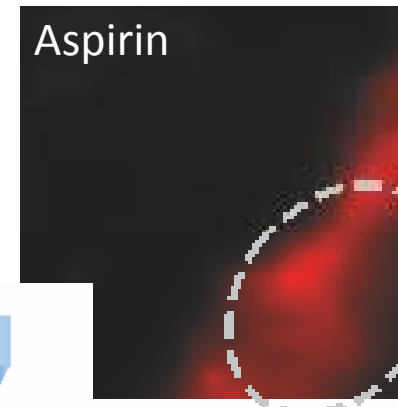
Raman mapping of a pharmaceutical tablet



AFM image topography
Total height variation: ~ 6 μm



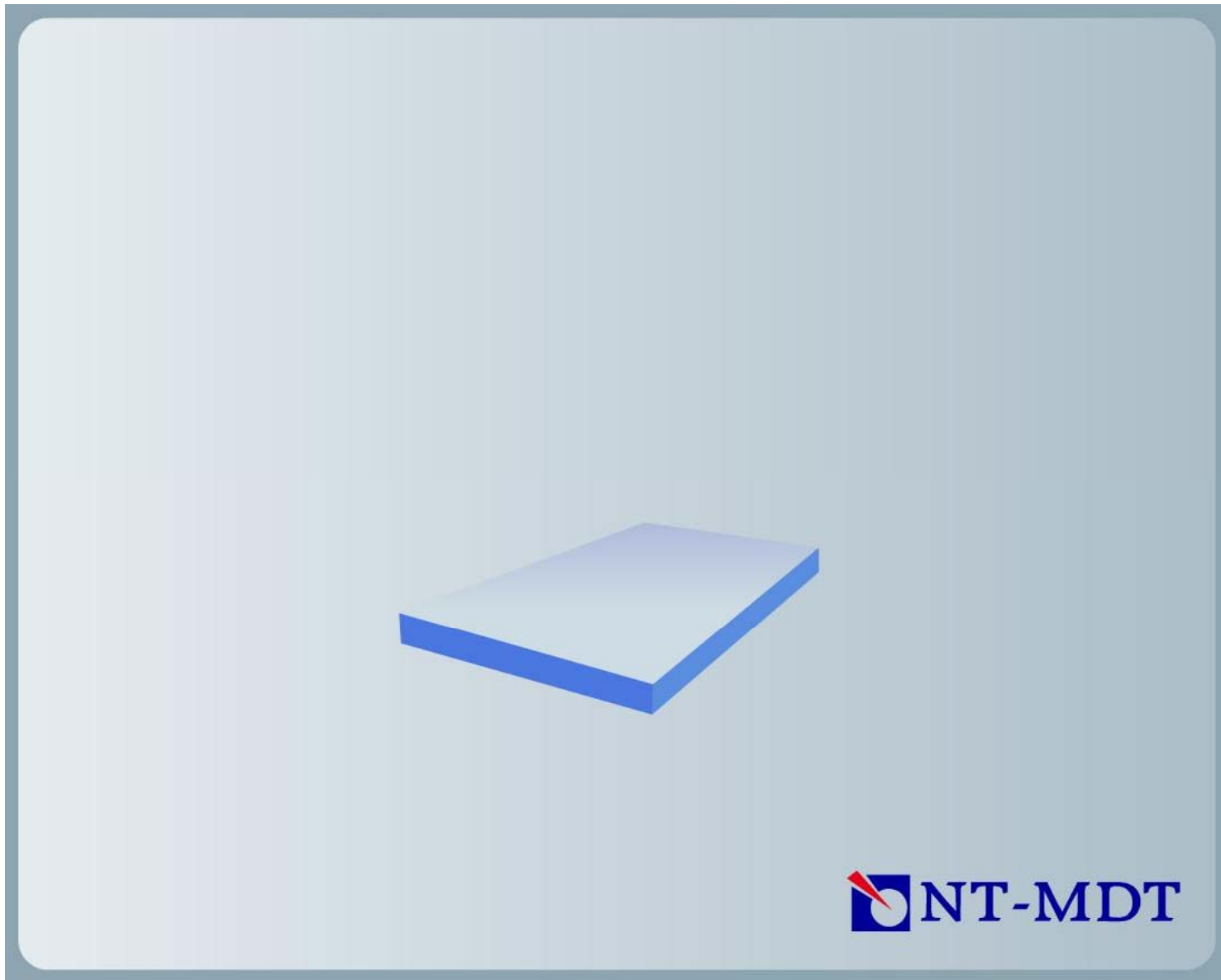
Raman maps
WITH focus track



Raman maps
WITHOUT focus track

Size of images: 20x20 μm

Graphene, AFM + Confocal Raman

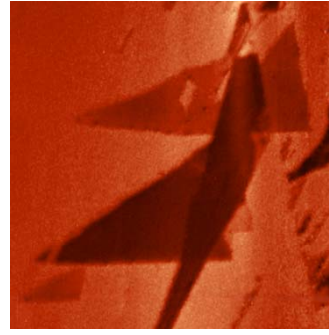


Real time simulation. Scanning area of 100x100 pixels, 50 sec scanning time

Graphene, AFM + Confocal Raman



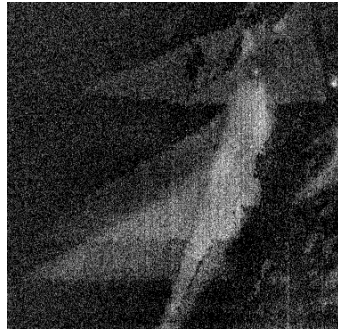
Lateral Force Microscopy
(friction)



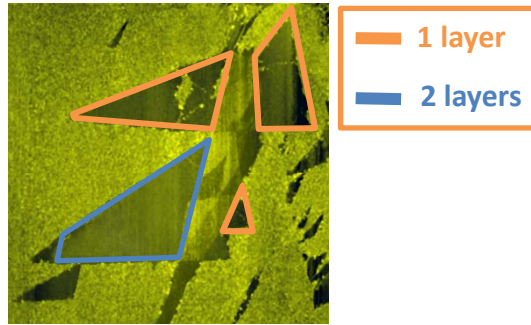
Electrostatic Force Microscopy
(charge distribution)



Force Modulation Microscopy
(elasticity)



Capacitance Microscopy

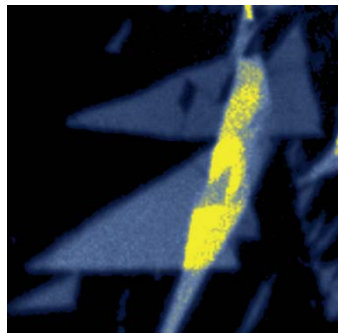


AFM Topography

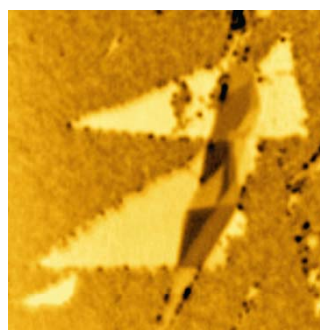
Size: 30*30 μm



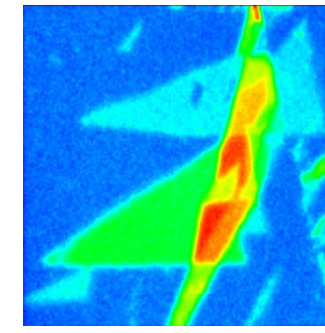
Scanning Kelvin Probe Microscopy
(surface potential)



Raman Map, 2D Band position

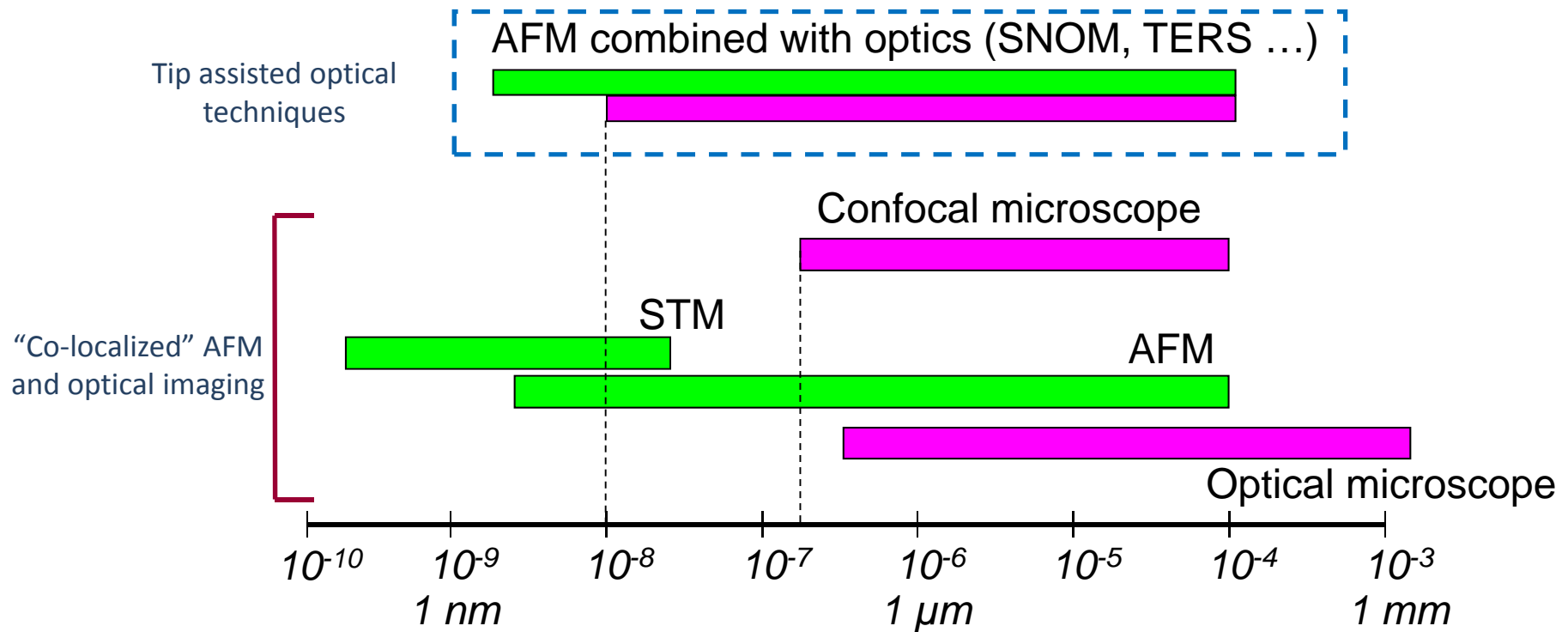


Confocal Rayleigh Microscopy



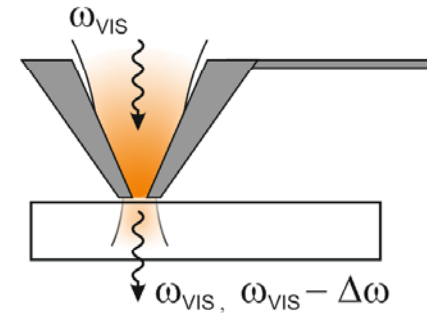
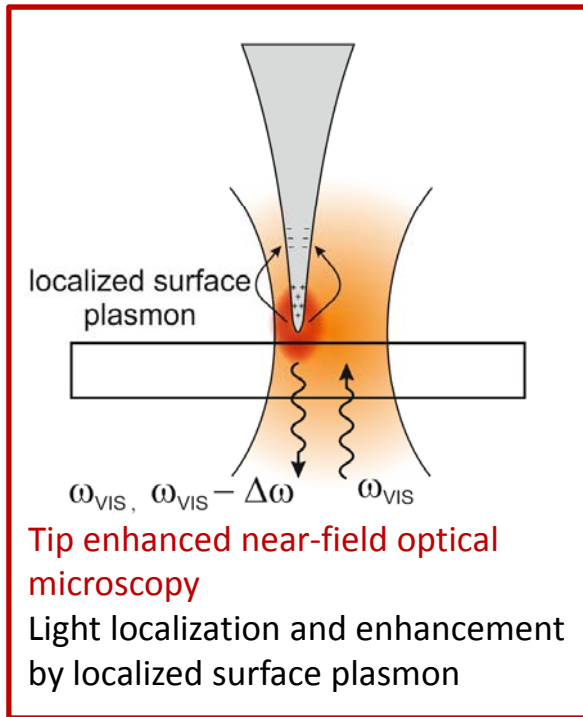
Raman Map, G-band Intensity

Resolution and capabilities of different techniques



-  Optical techniques (color imaging, physical & chemical analysis)
-  Scanning probe microscopy (topography, mechanical, electrical, magnetic and other properties of the surface)
-  AFM (STM) + Optical techniques = Dramatic increase of resolution and sensitivity

Super-resolution imaging using scanning optical antennas

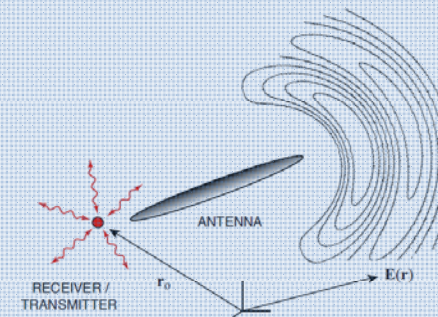


Aperture scanning near-field optical microscopy (SNOM)

Light transmission through non-resonant subwavelength aperture

Optical antenna: a device designed to efficiently convert free-propagating optical radiation to localized energy, and vice versa.

- L. Novotny, N. van Hulst, *Nature photonics* 5, 89 (2011)
- P. Bharadwaj, B. Deutch, L. Novotny, *Adv. In Opt. Phot.* 1, 438 (2009)
- Pohl D. W., *Optics, Principles and Applications* (World Scientific, 2000).



Localized surface plasmon resonance in metal nanoparticles (0D geometry)

$$\alpha = 4\pi R^3 \frac{\epsilon(\omega) - \epsilon_d}{\epsilon(\omega) + 2\epsilon_d}$$

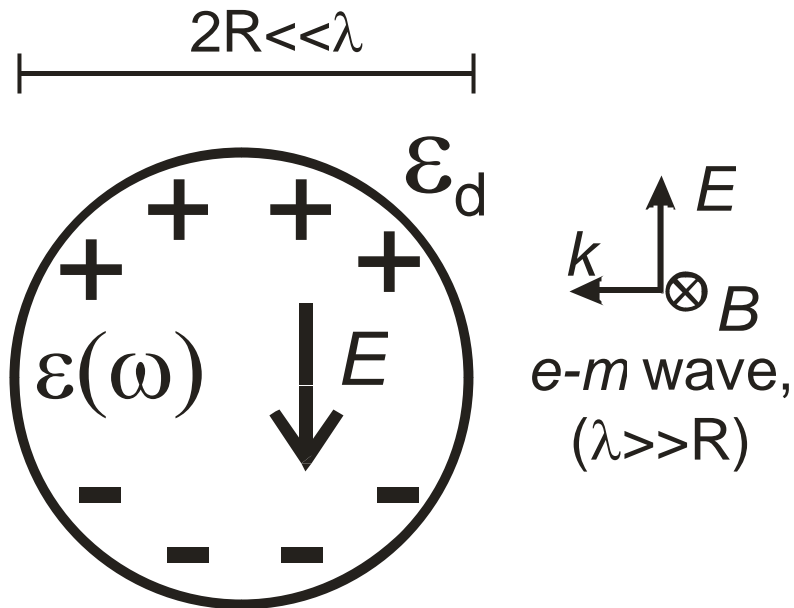
Nanoparticle polarizability

Resonant interaction with light at:

$$\epsilon(\omega_{res}) = -2\epsilon_d$$

(Fröhlich mode)

Drude model: $\epsilon'(\omega) = 1 - \omega_p^2 / \omega^2$



metal spherical nanoparticle
in dielectric medium

$$\omega_{pe} = \sqrt{\frac{4\pi n_e e^2}{m}}$$

$$\omega_{res} = \omega_p / \sqrt{3}$$

TERS: Importance of light polarization

“Z-polarized” light (with electrical field polarized along the tip axis) light experiences the largest enhancement at the tip apex

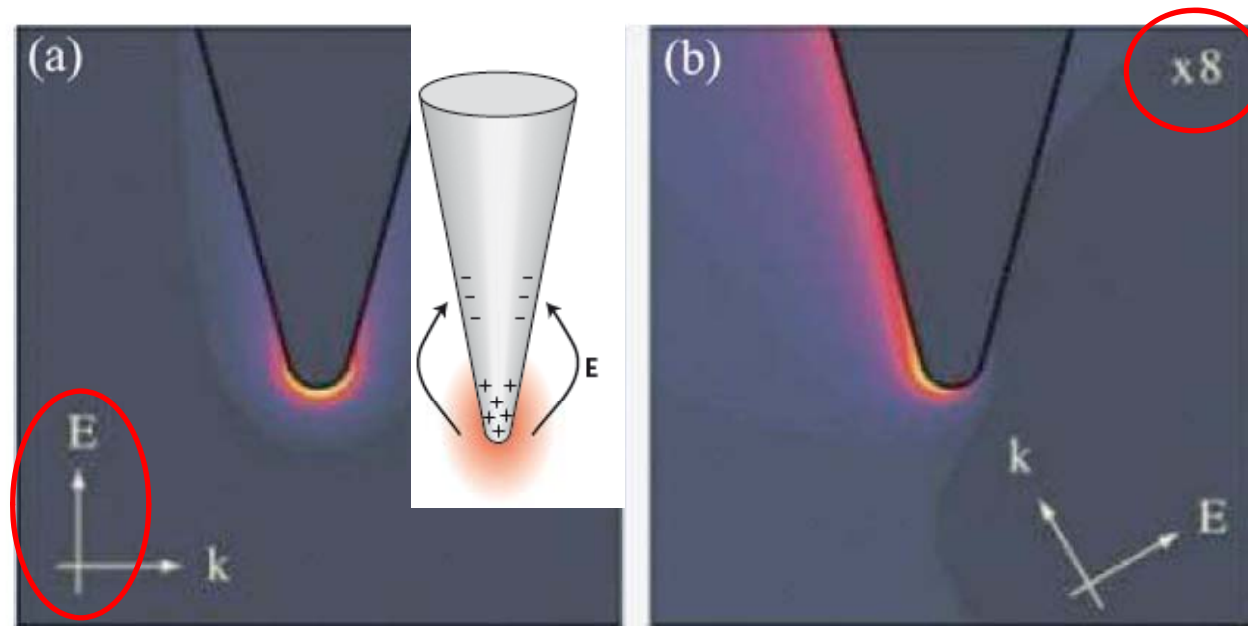


Fig. 1 Calculated field distribution at a sharp Au tip with a diameter of 5 nm. (a) Field distribution for an incident electric field vector parallel to the tip shaft showing localization of the electric field at the tip apex. (b) Field distribution for an incident electric field orientated nonparallel to the tip shaft. The field is no longer confined to the tip apex.

Taken from: N. Anderson, A. Hartschuh, L. Novotny, *Materials Today* (2005)

TERS enhancement factor as function of tip-sample distance

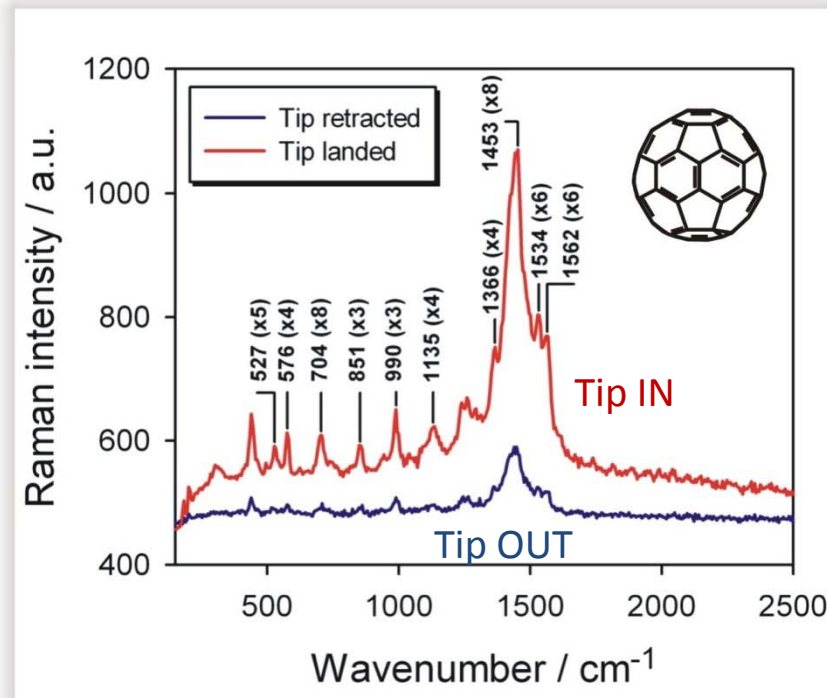
Fullerene thin film

Laser: 633 nm

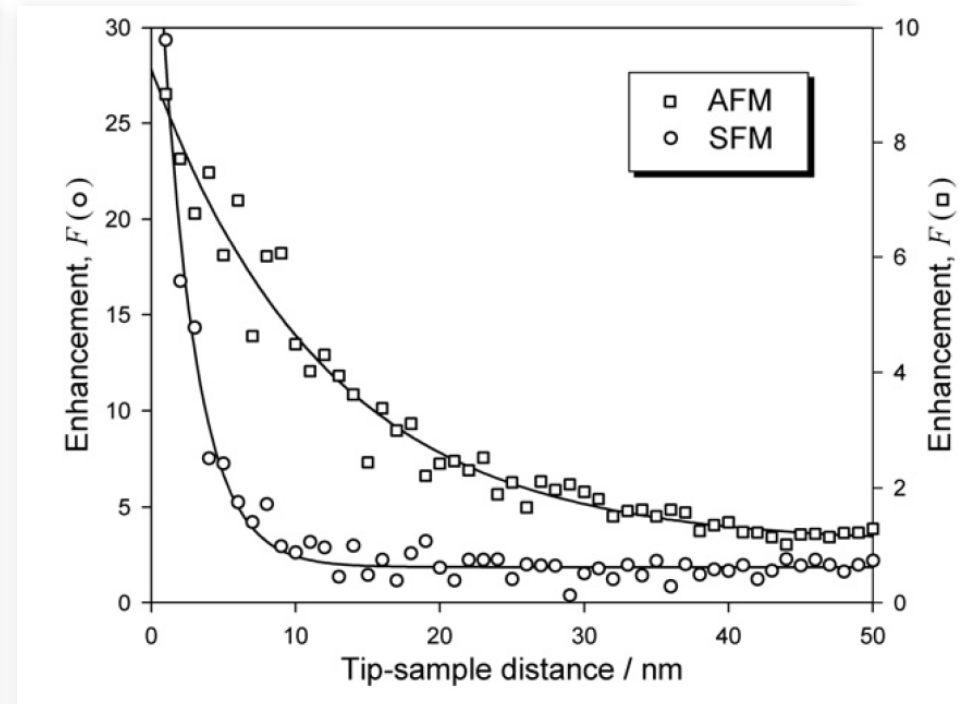
Tip: Au etched wire & Au coated cantilever

Mode: Shear force & non-contact mode

Enhancement factor: $\sim 5\text{--}10\text{x}$



Signal enhances >10 times after tip is approached



Signal enhancement versus tip-sample distance: proof of plasmonic near-field nature of the effect

Data courtesy of S. Kharintsev, J. Loos, G. Hoffman, G. de With, TUE, the Netherlands

TERS on carbon nanotubes

All data – using NT-MDT instrument

Tip Enhanced Raman Scattering ("nano-Raman") imaging

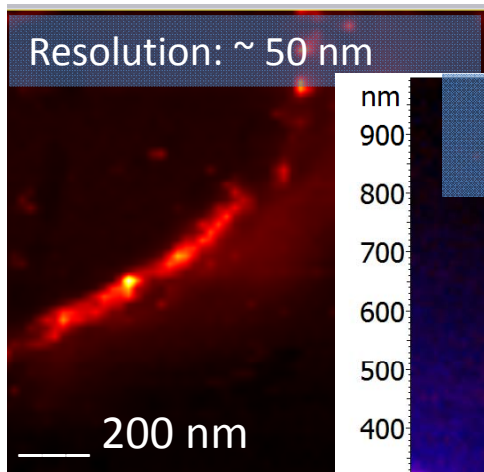


 NT-MDT

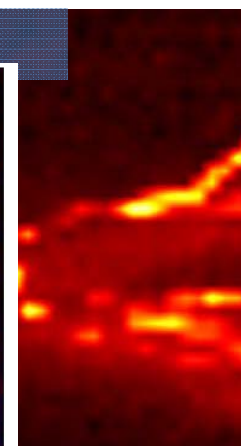
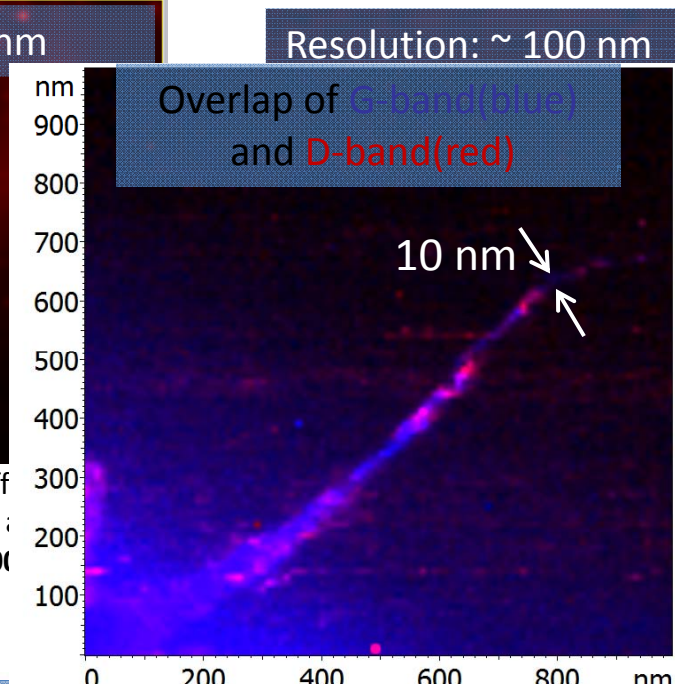


TERS on carbon nanotubes

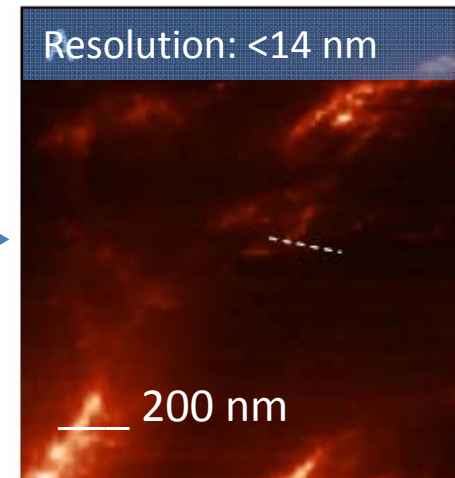
All data – using NT-MDT instrument



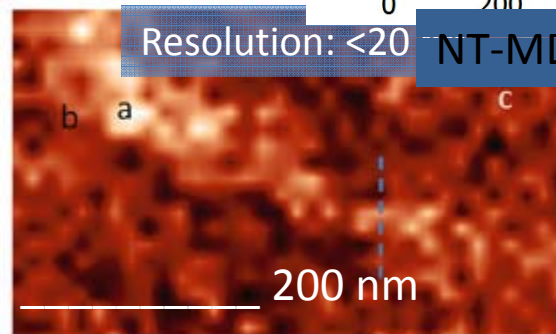
S.S. Kharintsev, G. Hoffmann, G. Dorozhkin, G. de With, *Nanotechnology* 18 (2007) 175701



S.S. Kharintsev, G. Hoffmann, G. Dorozhkin, G. de With, *Nanotechnology* 18 (2007) 175701

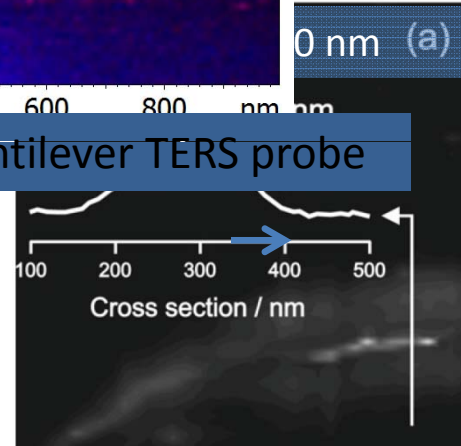


Chan K.L., Kazarian S.G., *Nanotechnology* 21, 445704 (2010)

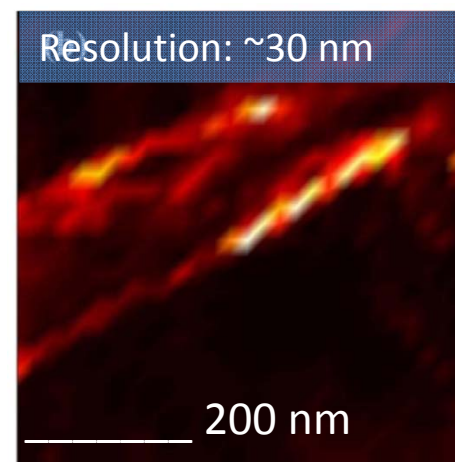


Chan K.L., Kazarian S.G., *Nanotechnology* 22, 175701 (2011)

NT-MDT, Cantilever TERS probe

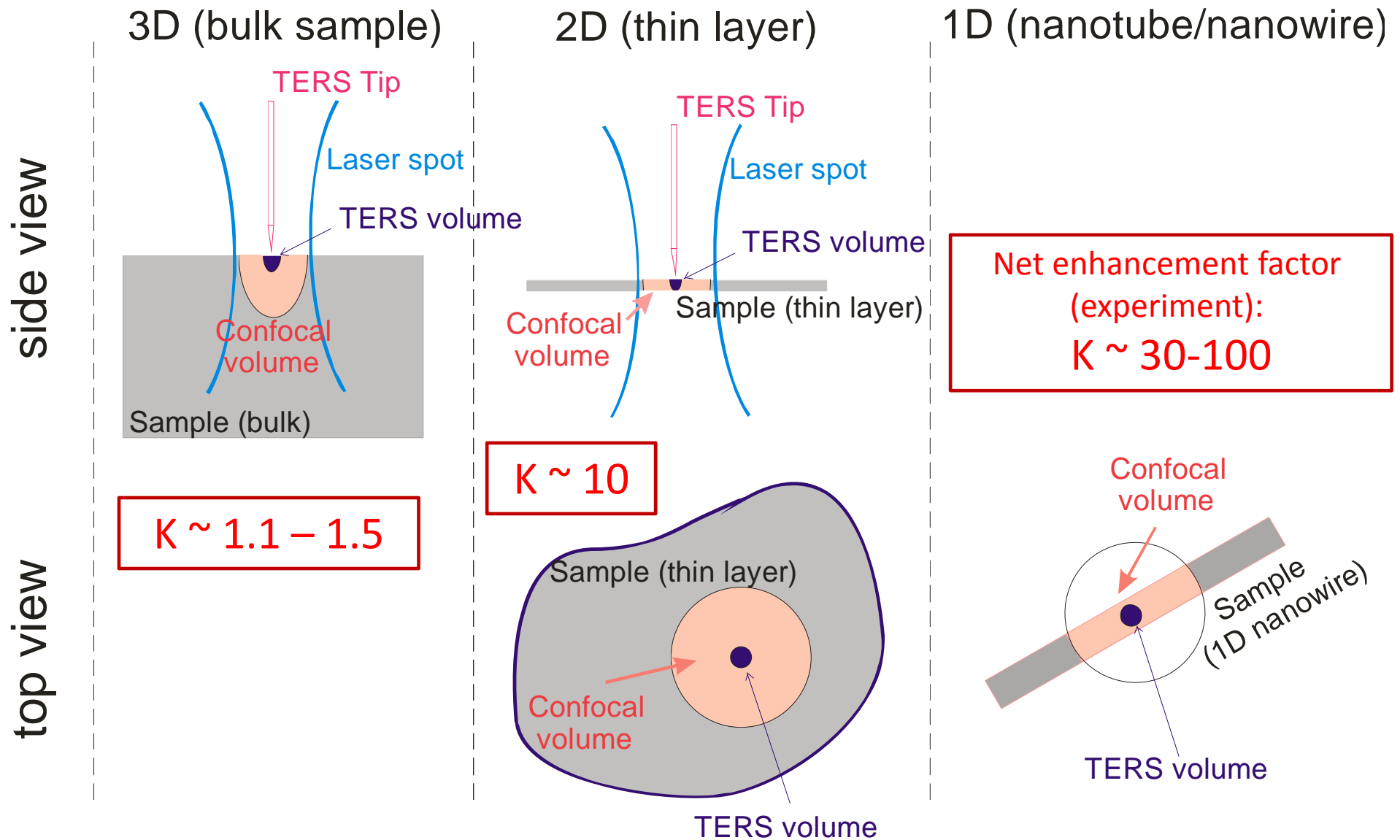


S. Kharintsev, G. Hoffmann, A. Fishman. & M. Salakhov *J. Phys. D: Appl. Phys.* 46 (2013) 145501



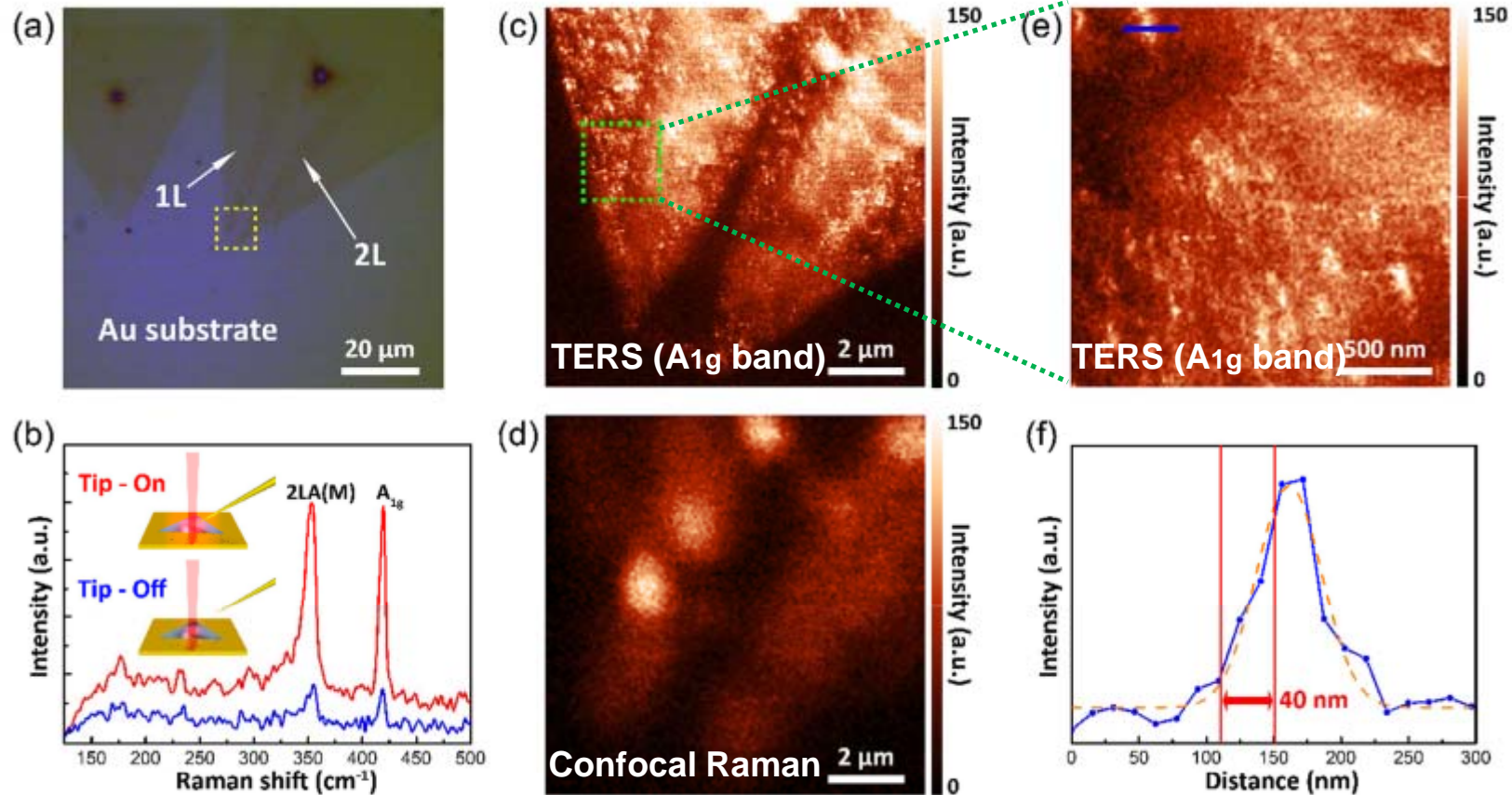
M. Zhang, J. Wang, Q. Tian, *Optics Communications* 315, 164 (2014)

TERS enhancement in different geometries (1D, 2D, 3D)



Far field to near field volume ratio decreases with decreasing dimension – lower dimensions are more advantageous for TERS

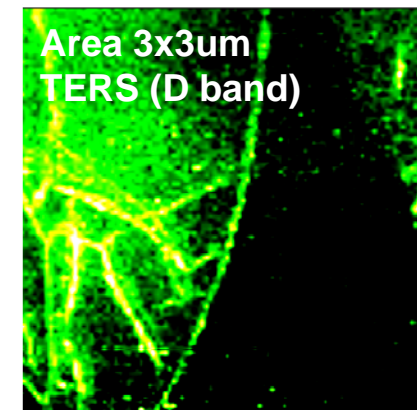
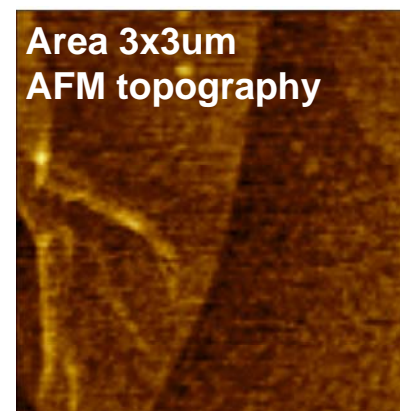
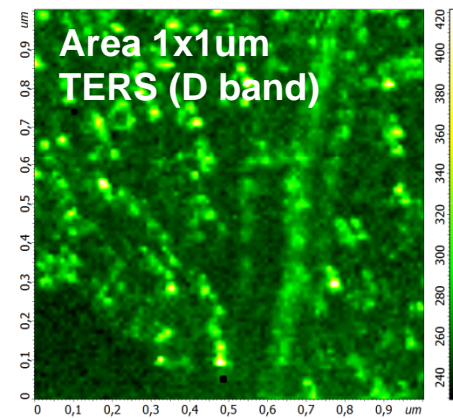
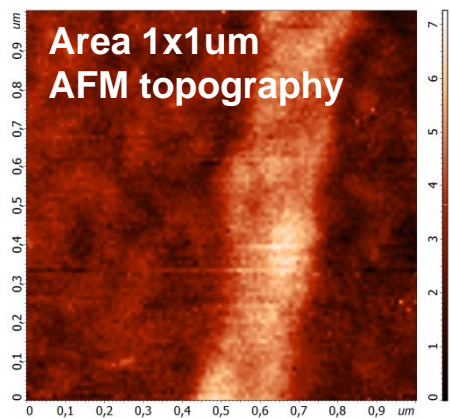
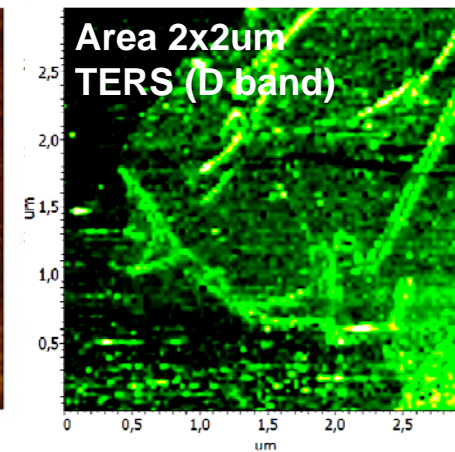
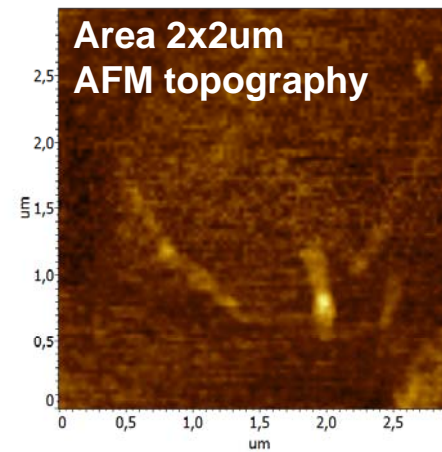
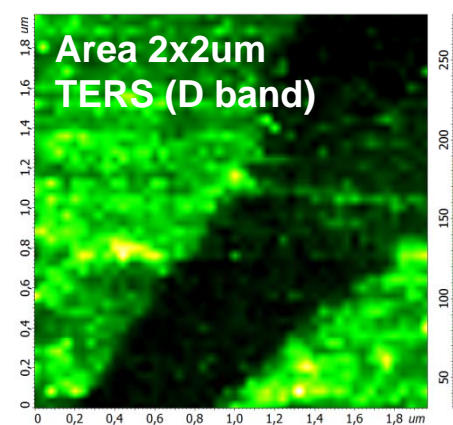
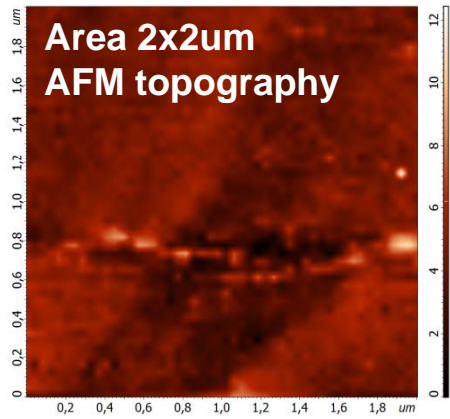
TERS spectra and images of mono/bilayer WS₂ flake



C. Lee *et al.*, "Tip-Enhanced Raman Scattering Imaging of Two-Dimensional Tungsten Disulfide with Optimized Tip Fabrication Process," *Sci. Rep.*, vol. 7, no. September 2016, p. 40810, Jan. 2017.

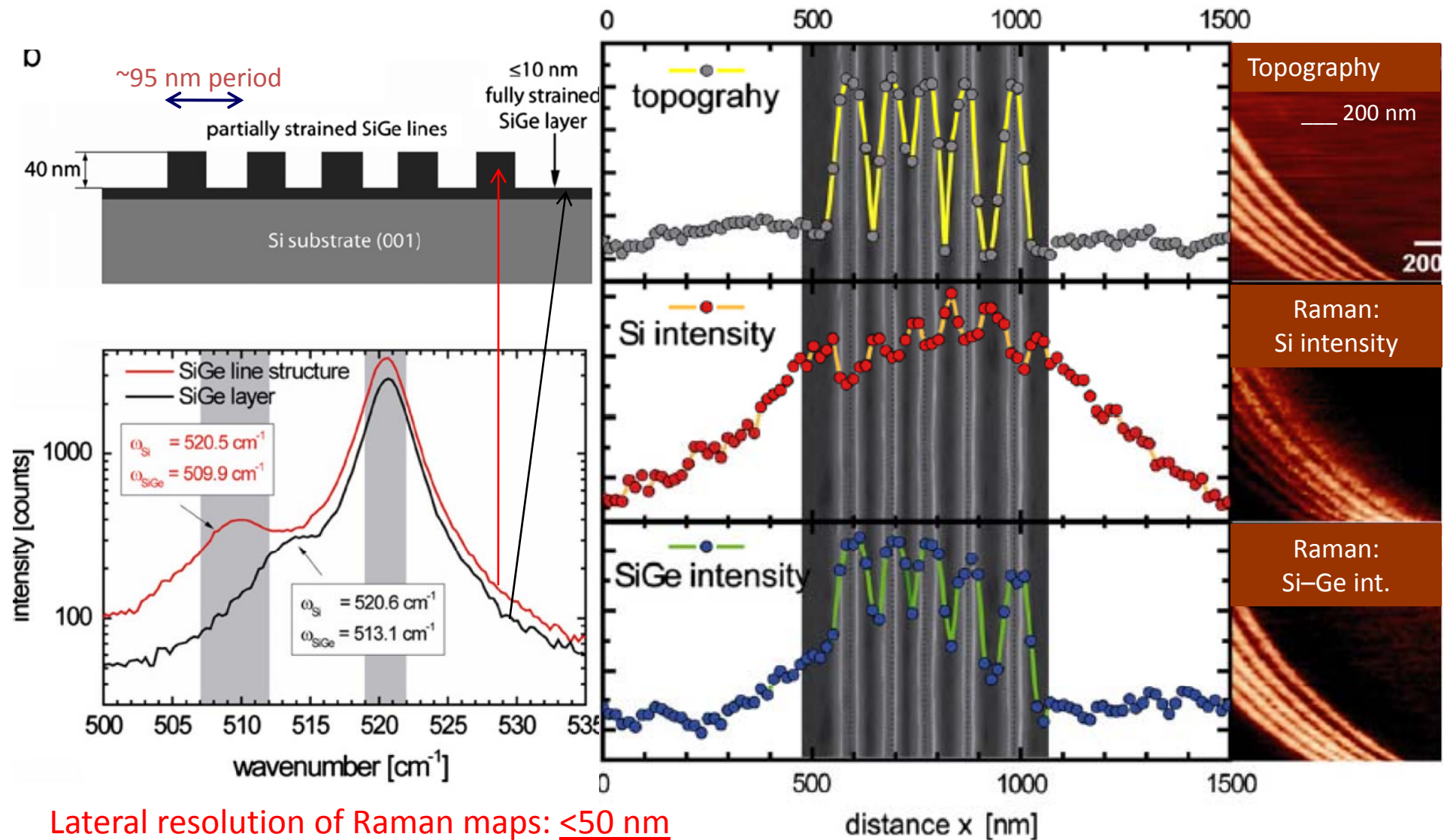
TERS on Graphene Oxide

AFM TERS cantilevers, HYBRID regime



Typical TERS resolution with AFM TERS probes: ~ 20 – 40 nm.

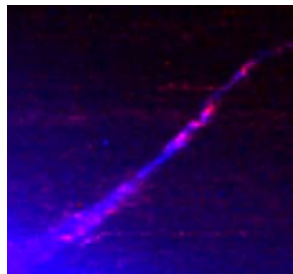
TERS (“nano-Raman”) on periodic Si-Ge structure resolution ~50 nm



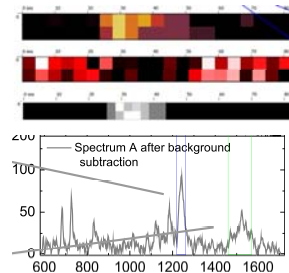
Lateral resolution of Raman maps: <50 nm

Tip Enhanced Raman Scattering

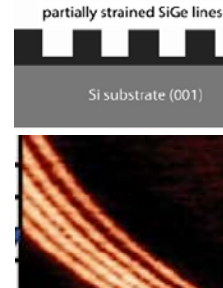
Various types samples. Proven by multiple publications by NT-MDT customers.



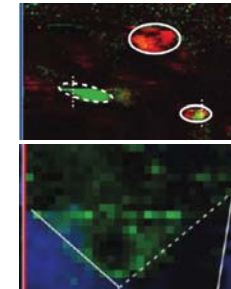
Carbon nanotubes
Resolution: ~10 nm
Nanotechnology, 2011
& ~10 other papers



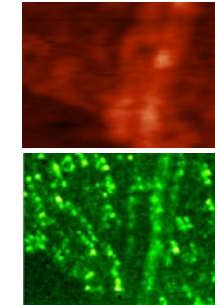
DNA molecule
Resolution: ~15 nm
Ang. Chem. Int., 2014,
E. Lipiec et. al



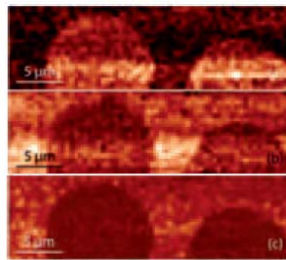
Si/SiGe structures
Resolution: <50 nm
Ultramicroscopy, 2011
P. Hermann et al.



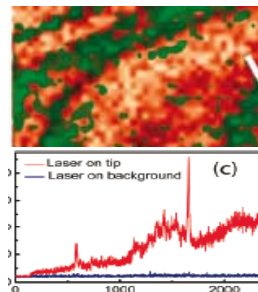
Graphene
Resolution: ~12 nm
ACS Nano, 2011
R. Zenobi et. al.



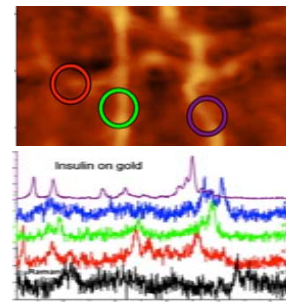
Graphene Oxide
Resolution: ~15 nm
A. Shelaev, et. al.,
2014



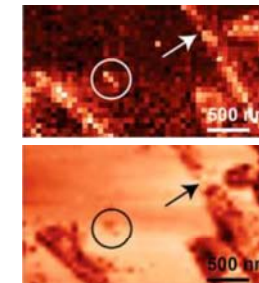
Thiol monolayers
Resolution: ~50 nm
Beilstein J. Nano, 2011
R. Zenobi et. al.



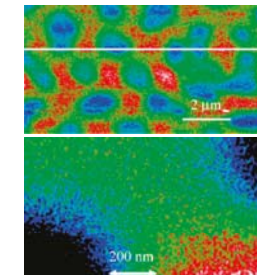
Thin molecular layers
Resolution: ~15 nm
NanoLett., 2010
R. Zenobi et. al.



Amyloid fibrils
Resolution: ~50 nm
Plasmonics, 2012
E. Di Fabrizio et. al.



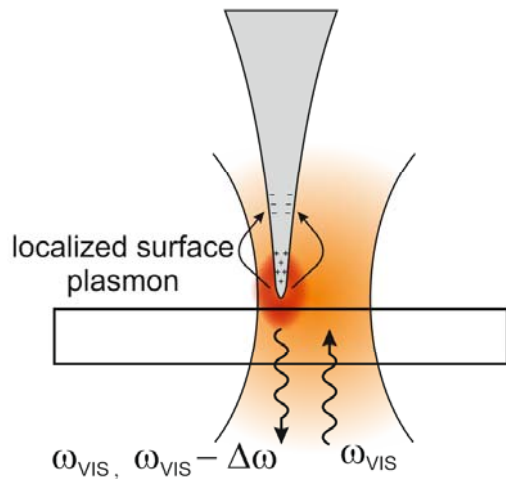
Peptide nanotapes
Resolution: ~50 nm
ACS Nano, 2013
R. Zenobi et. al.



Polymers
Resolution: ~50 nm
Macromol., 2011
G. Hoffmann et al.

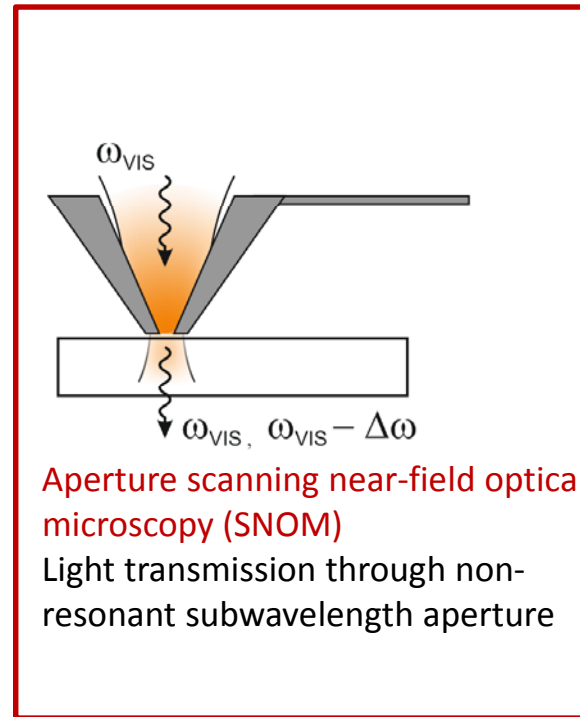
More than 50 publications.

Super-resolution imaging using scanning optical antennas



Tip enhanced near-field optical microscopy

Light localization and enhancement by localized surface plasmon

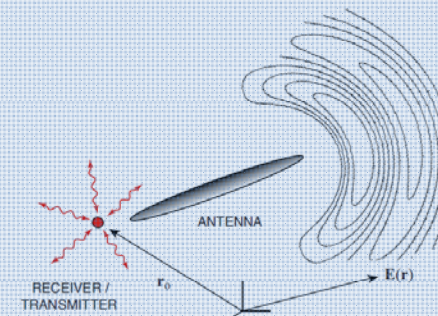


Aperture scanning near-field optical microscopy (SNOM)

Light transmission through non-resonant subwavelength aperture

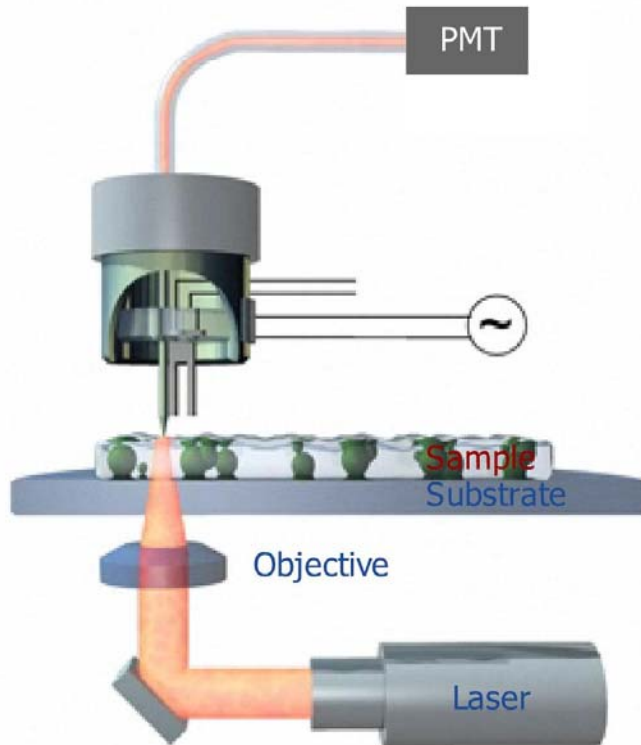
Optical antenna: a device designed to efficiently convert free-propagating optical radiation to localized energy, and vice versa.

- L. Novotny, N. van Hulst, *Nature photonics* 5, 89 (2011)
- P. Bharadwaj, B. Deutch, L. Novotny, *Adv. In Opt. Phot.* 1, 438 (2009)
- Pohl D. W., *Optics, Principles and Applications* (World Scientific, 2000).



Two major types of SNOM

FIBER SNOM

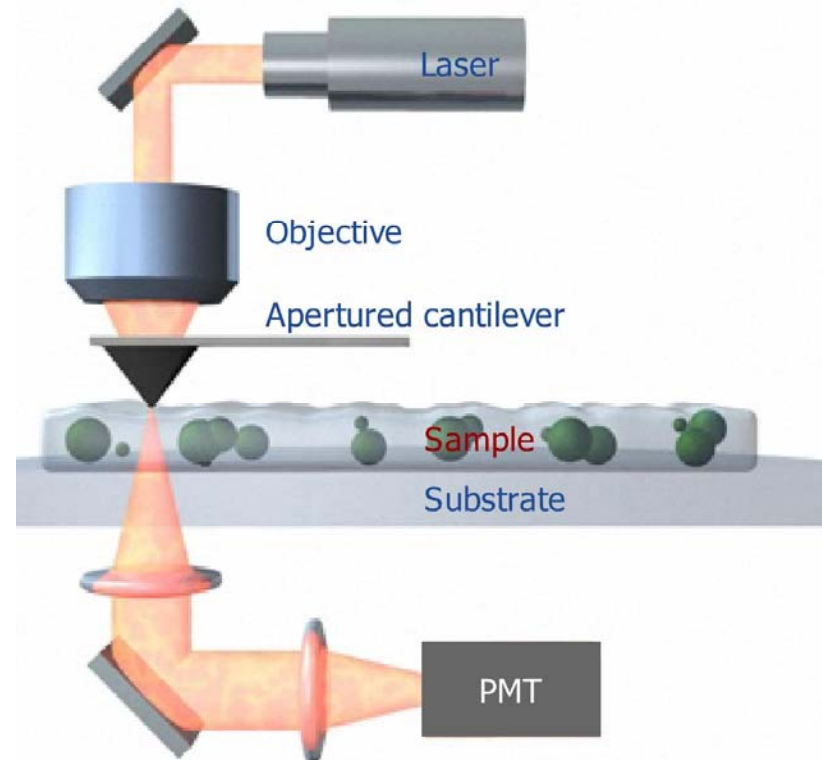


Copyright © NT-MDT

www.ntmdt.com

Example shows
SNOM collection mode
(laser signal)

CANTILEVER SNOM

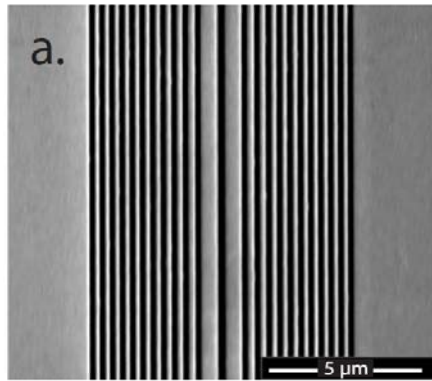


Copyright © NT-MDT

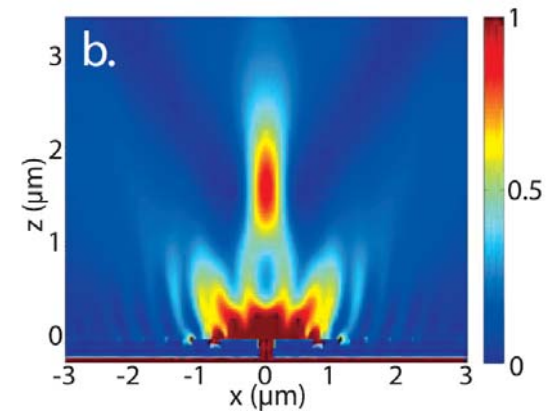
www.ntmdt.com

Example shows
SNOM Transmission mode
(laser signal)

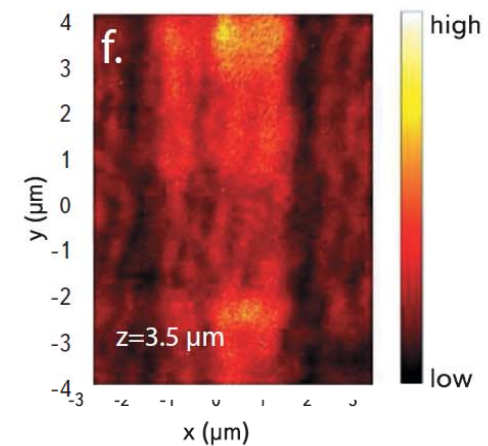
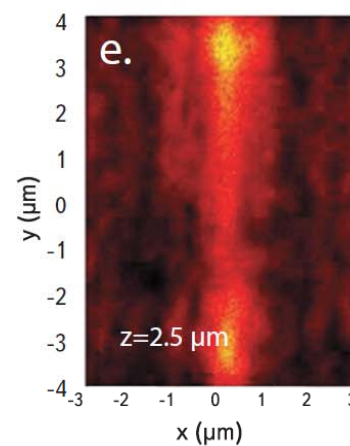
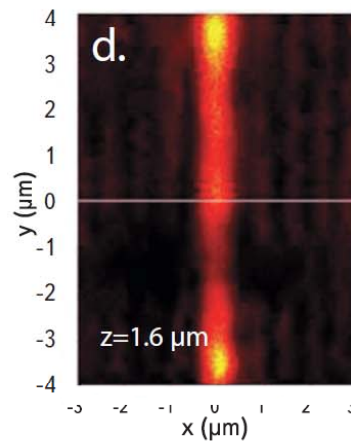
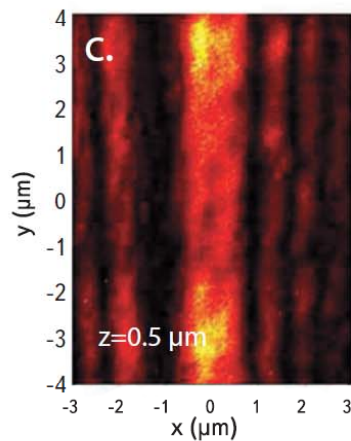
SNOM for focusing micro-devices



SEM image of a focusing plasmonic device



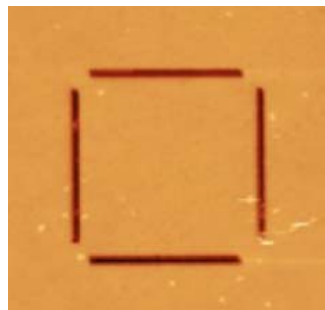
Intensity distribution of the transmitted/focused light (simulation)



SNOM data: light intensity at different distances from the sample surface

Data from: Dr. Fenghuan Hao, Dr. Rui Wang and Dr. Jia Wang, OPTICS EXPRESS Vol. 18, No. 3, 15741- 15746 (2010)

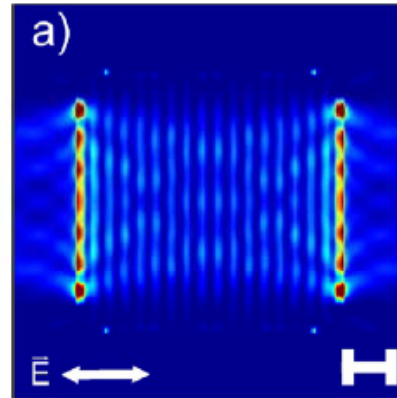
SPP interference studied by SNOM



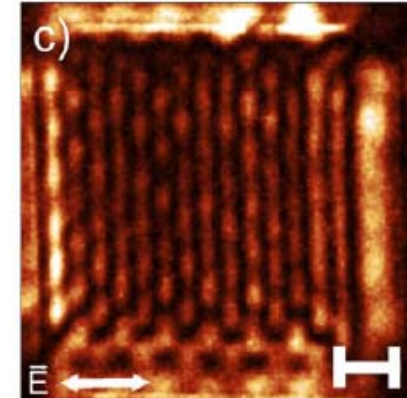
Slit structure in Au film (AFM image)

Excitation light polarization →

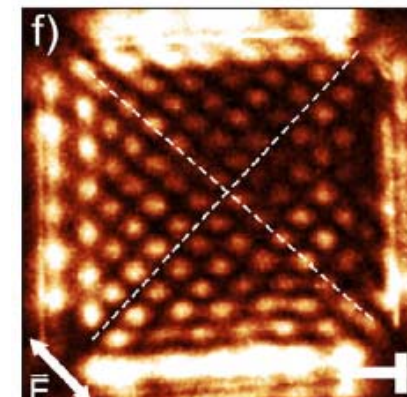
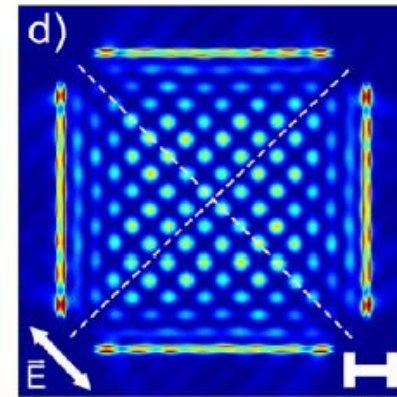
Numerical simulation



Experiment



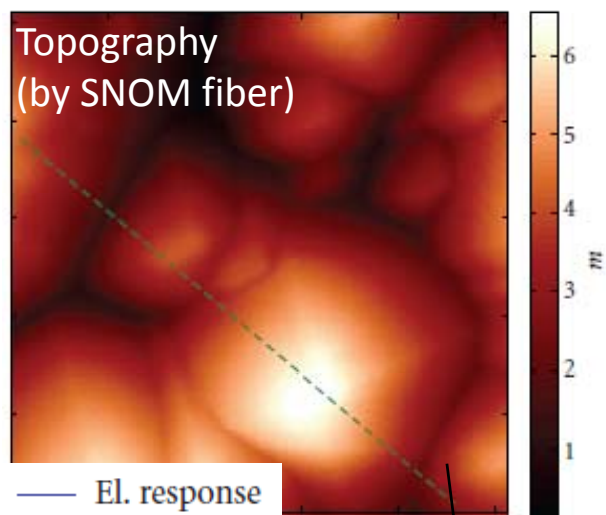
Excitation light polarization →



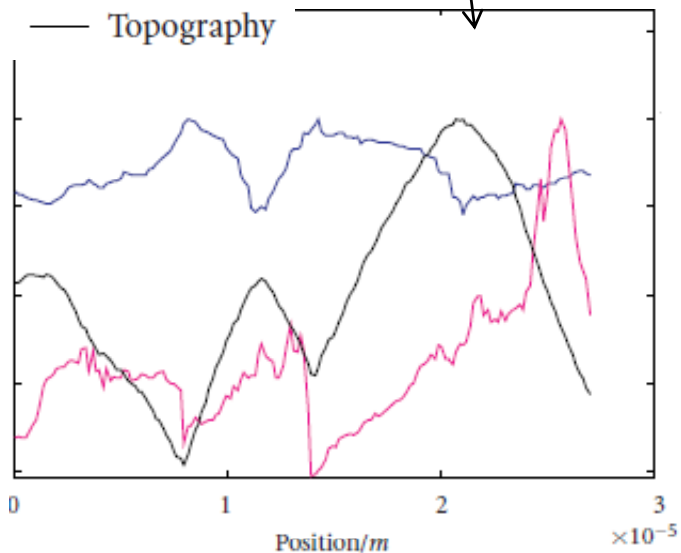
Near-field interference pattern of surface plasmon polaritons
in a square-like slit structure in Au film

Control and Near-Field Detection of Surface Plasmon Interference Patterns.
Petr Dvořák, Tomáš Neuman, Tomáš Šikola et al., Nano Letters 2013

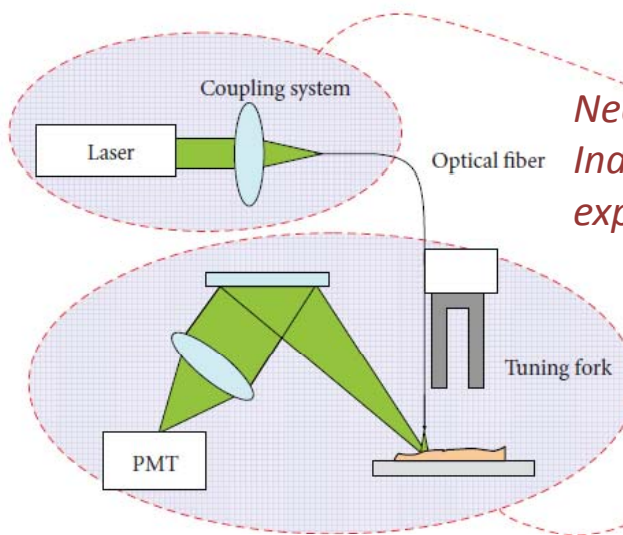
SNOM for localized optical excitation in photovoltaics



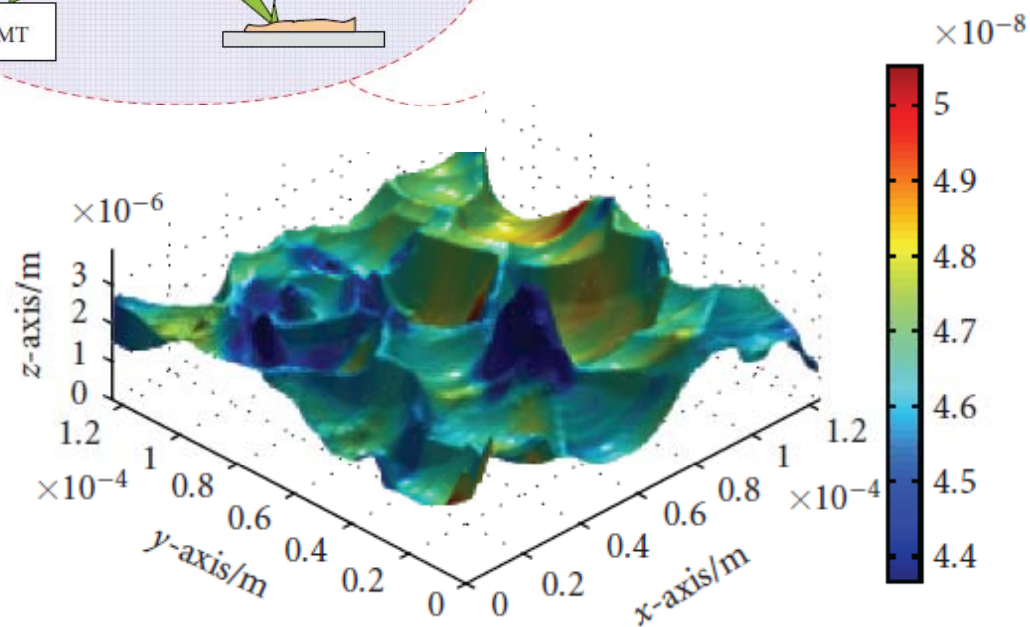
— El. response
— Reflection
— Topography



Correlation of local reflectivity, local light-current conversion and topography



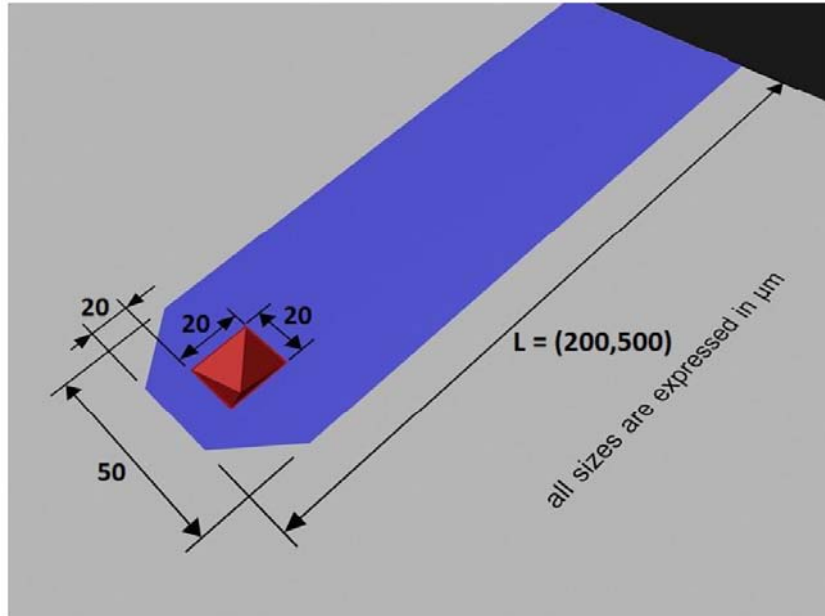
Near-Field Optical Beam Induced Photocurrent (NOB-IC) experiment



Overlay of topography (3D) and local light to current conversion coefficient (color)

NT-MDT cantilever SNOM: contact AND non-contact probes

1) Lever sizes and the pyramid position:

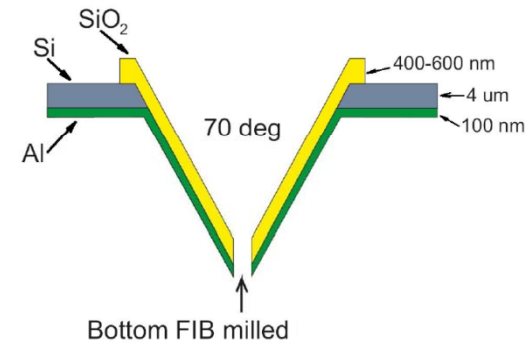


Pyramid LxWxH = 20x20x13 (70 deg)

	Spring Constant (N/m)			Frequency (kHz)			Length (micron)			Width (micron)			Thickness (micron)		
	Nominal	Min	Max	Nominal	Min	Max	Nominal	Min	Max	Nominal	Min	Max	Nominal	Min	Max
NonContact	16.5	5.9	39.0	130	88	180	200	190	210	55	54	57	4	3	5
Contact	1.01	0.41	2.30	20.8	15	27	500	490	510	55	54	57	4	3	5

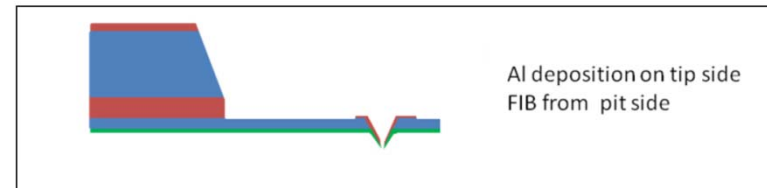
Probe	Resolution	TR@ 473
1 contact	150 nm	$\sim 3 \cdot 10^{-4}$
1 contact	???	$0.3 \cdot 10^{-4}$
1 noncontact	110 nm	$\sim 0.16 \cdot 10^{-4}$
2 noncontact	120 nm	$\sim 0.5 \cdot 10^{-4}$
3 noncontact	135 nm	$\sim 0.7 \cdot 10^{-4}$
4 noncontact	100 nm	$\sim 0.2 \cdot 10^{-4}$
5 noncontact	150 nm	$\sim 1.6 \cdot 10^{-4}$

2) Tip shape and aperture size:

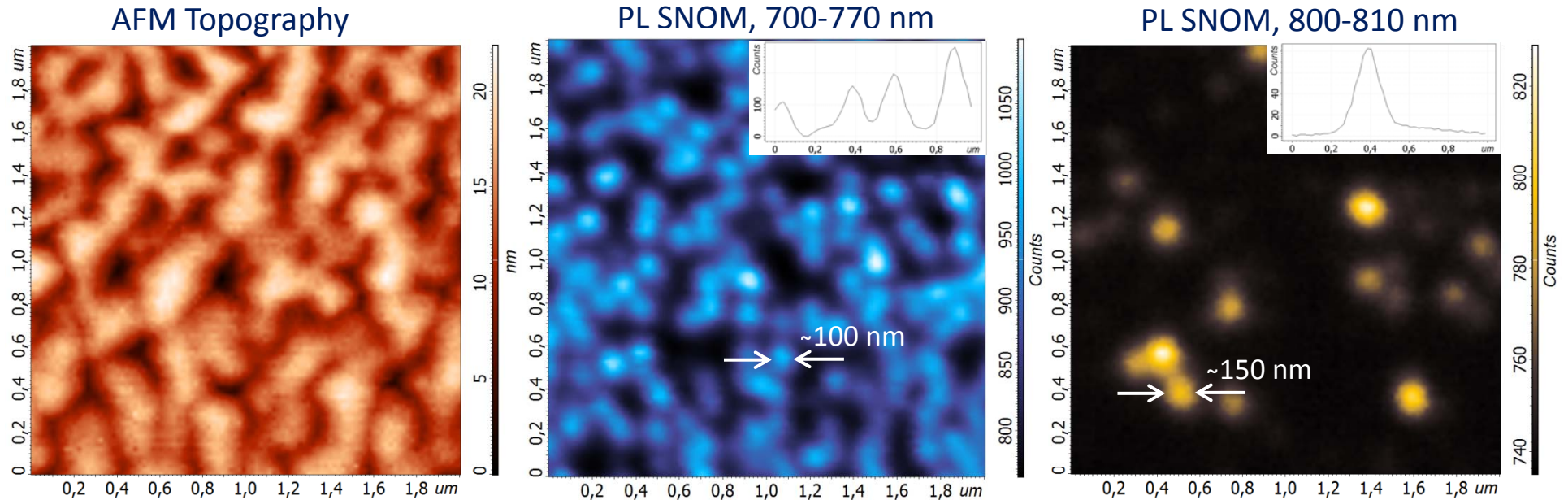


Pyramid (SiO₂) thickness 400-600 nm

3) Coating: Al, about 100 nm, coating from bottom side. Bottom FIB milling is done after coating. Typical aperture diameter about 170 ± 25 nm.



SNOM of InP/GaInP quantum dots with GaInP cap layer



Cap layer only (QDs not visible)

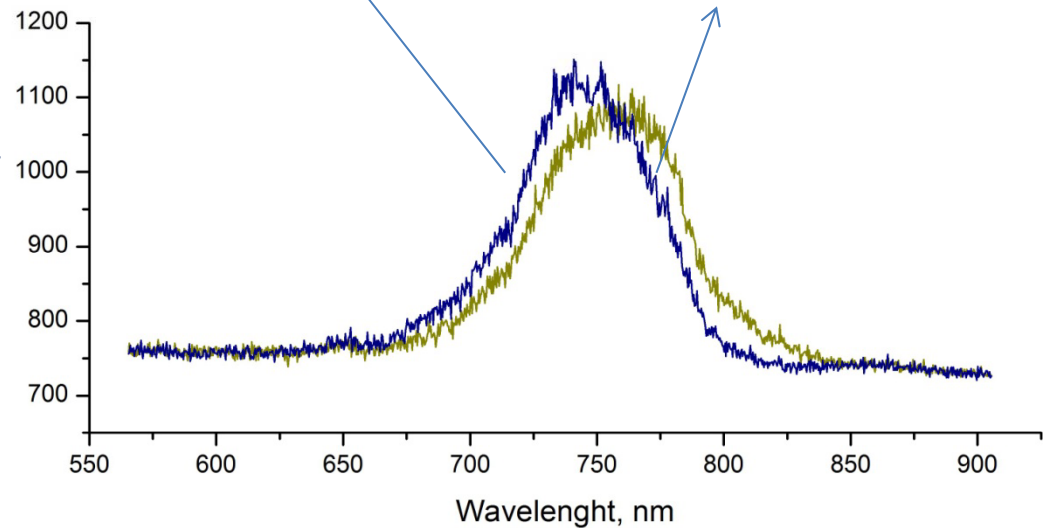
2x2 μm scans

Simultaneously obtained topography (left) and SNOM maps of photoluminescence (PL) in 700-770 nm (center) and 800-810 nm (right) spectral regions. 100x100 pixels, 0.1 s/point

Images obtained by cantilever based SNOM in with excitation and collection via the same SNOM aperture

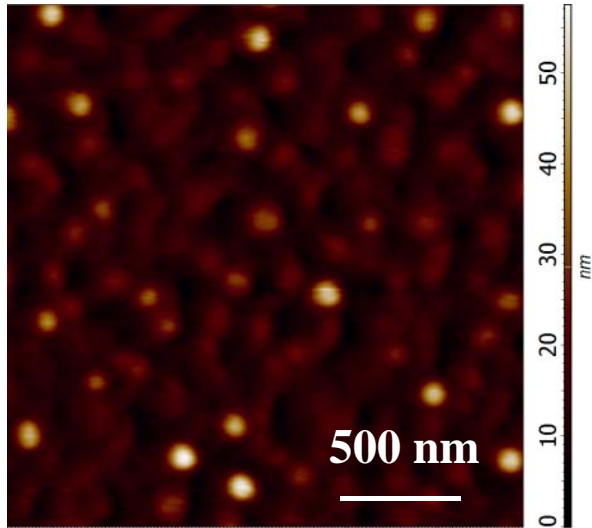
20-50 nm dia. QDs

100-200 nm dia. QDs

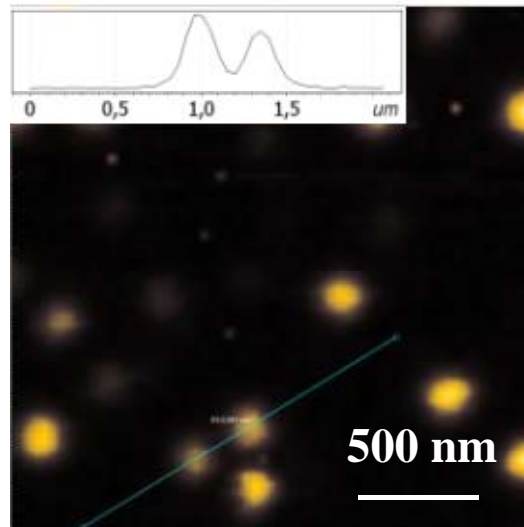


QD SNOM spectroscopy and topography

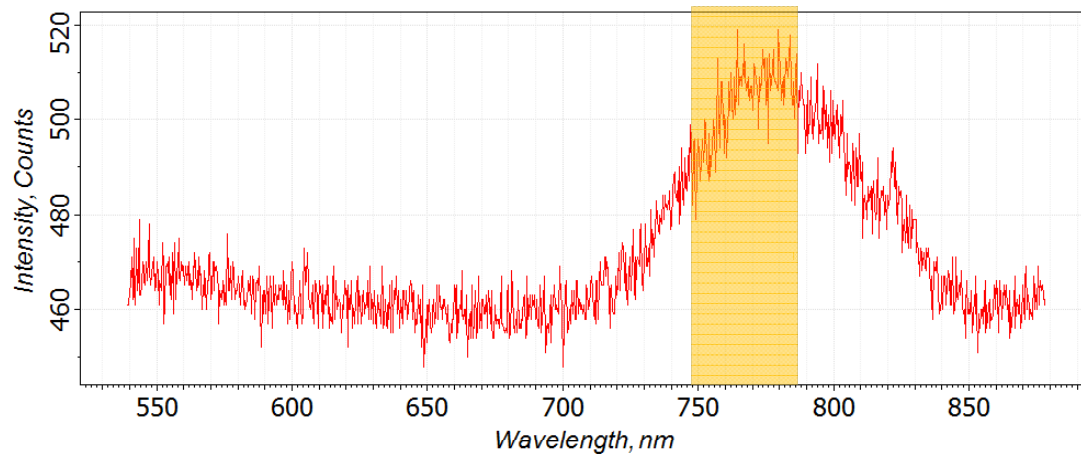
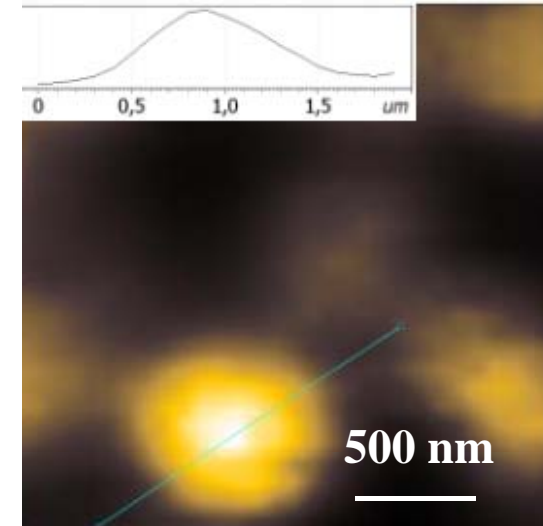
AFM Topography



SNOM PL, 750-780 nm



Confocal map, 750-780 nm

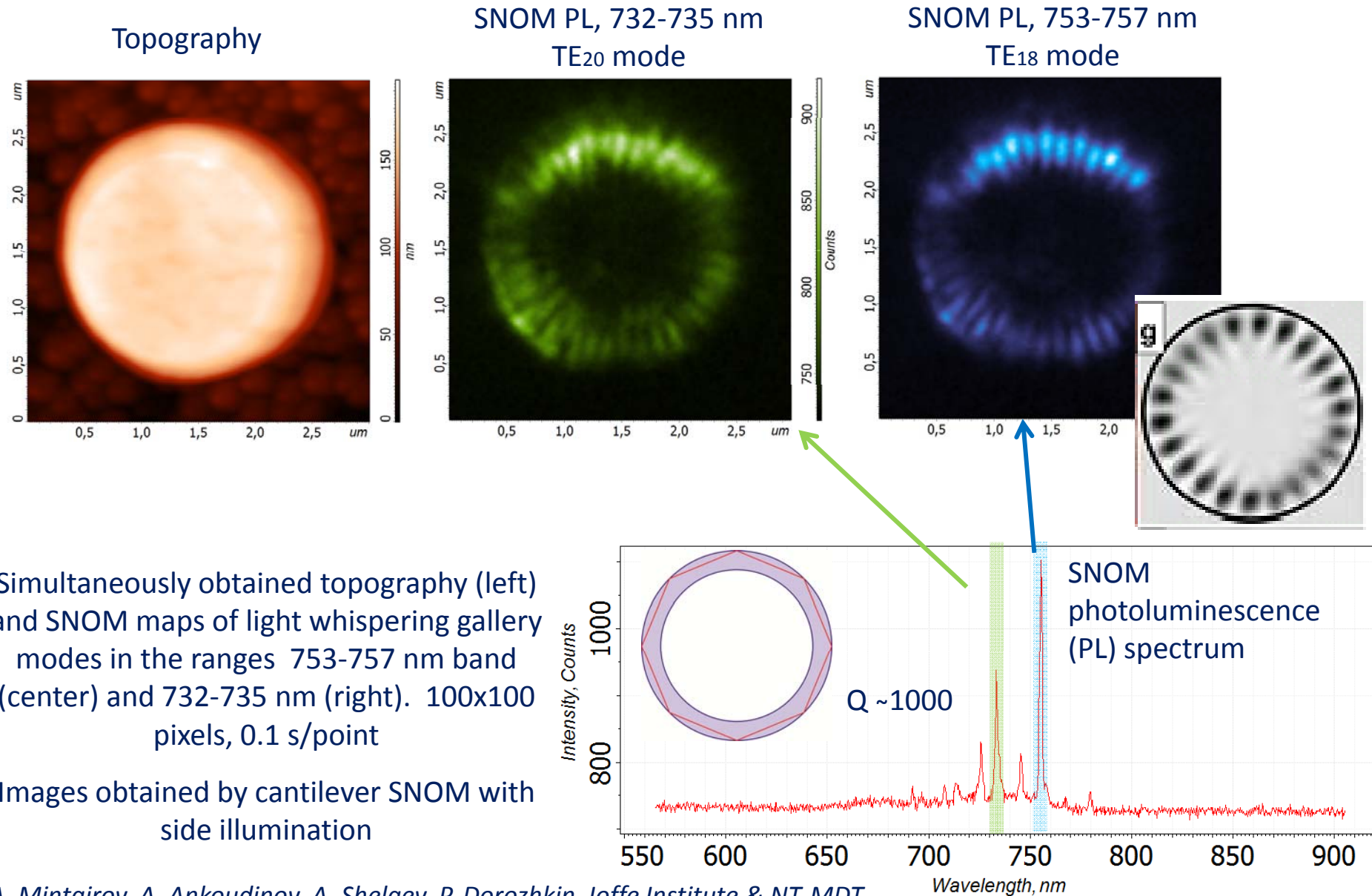


3x3 μm scans

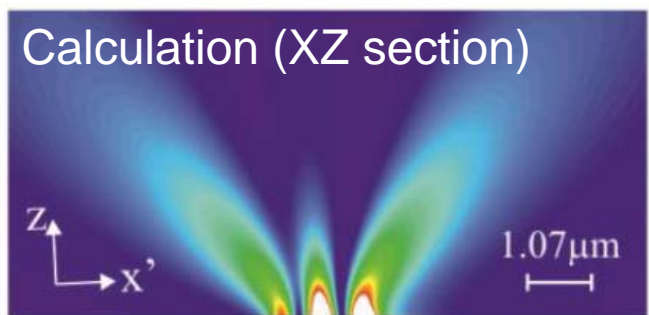
Simultaneously obtained topography (left) and SNOM maps of photoluminescence (PL) in 750-780 nm band (center) and confocal map with the same spectral band (right). 100x100 pixels, 0.1 s/point. Images obtained by cantilever based SNOM in with excitation and collection via the same SNOM aperture. AFM tapping mode used.

Shelaev A. V., Mintairov A. M., Dorozhkin P. S., and Bykov V. A. Scanning near-field microscopy of microdisk resonator with InP/GaN quantum dots using cantilever-based probes // J. Phys. Conf. Ser. 2016. Vol. 741. P. 12132.

Whispering gallery light modes in microdisks with InP/GaInP self-organized quantum dots



Laser emission in 3D studied by SNOM



Cantilever SNOM operation at near IR region ($\sim 1.1 \mu\text{m}$)

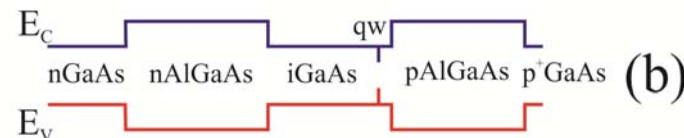
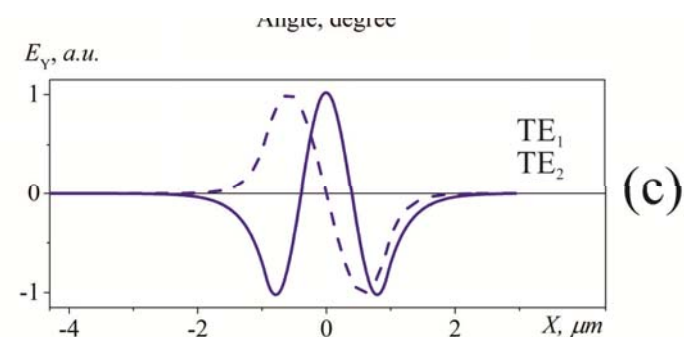


← Far field (propagating e-m radiation)



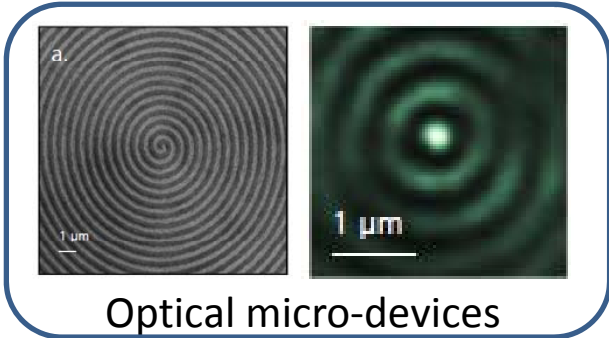
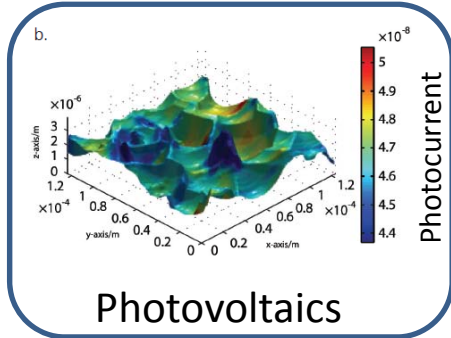
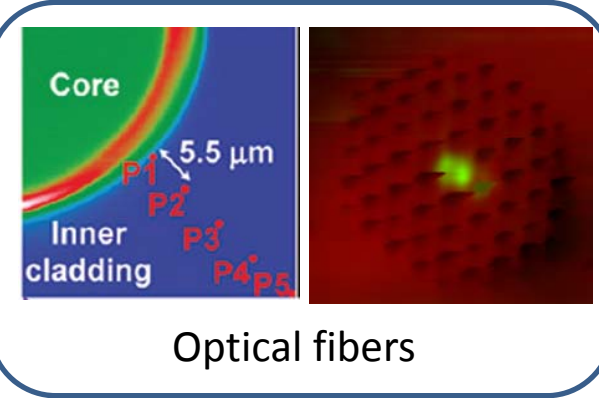
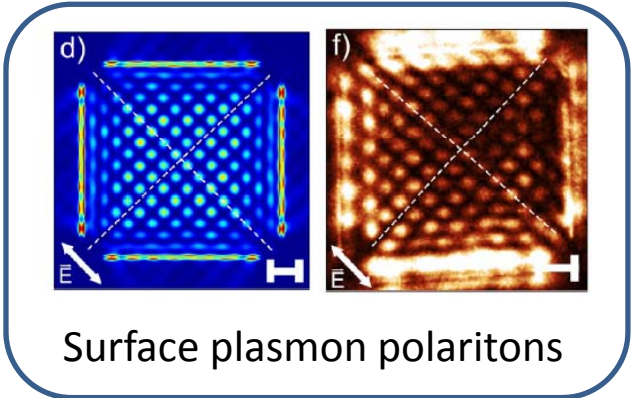
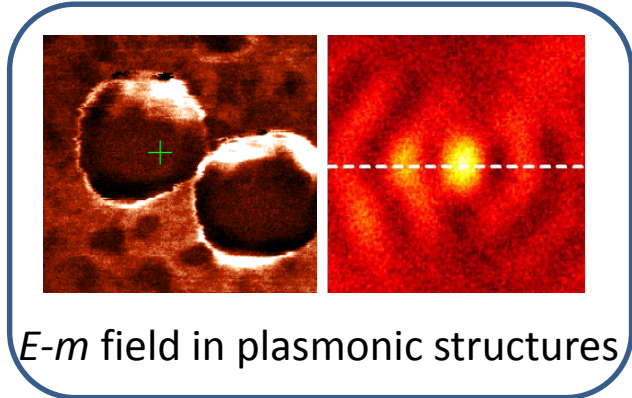
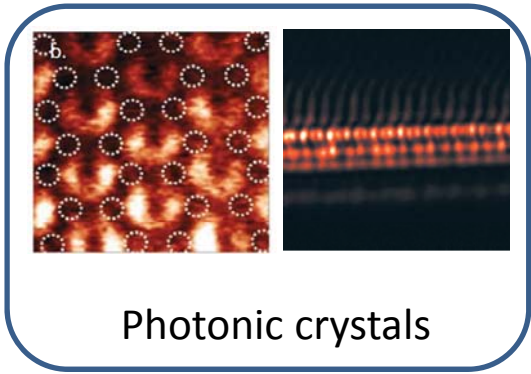
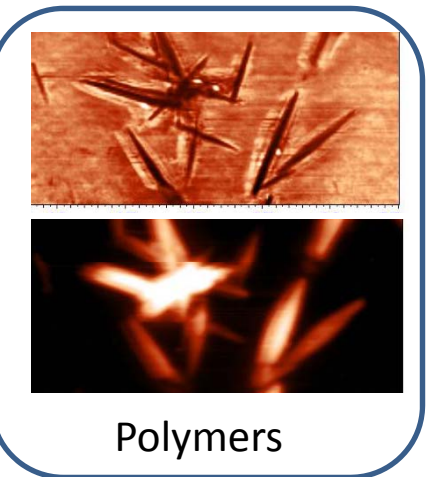
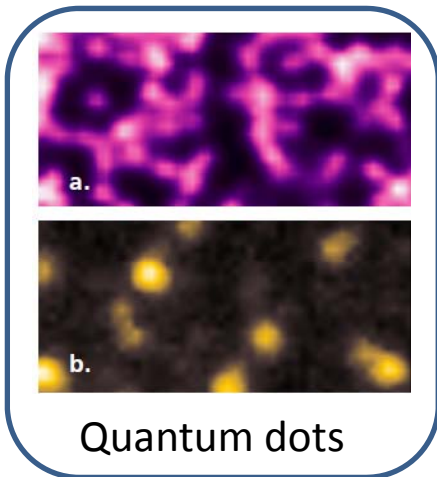
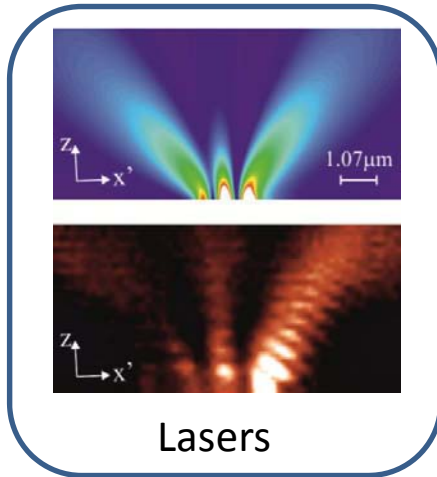
← Surface (near field)

← Surface (near field)



A.V. Ankudinov, P.S. Dorozhkin, A.A. Podoskin, A.V. Shelaev, S.O. Slipchenko, I.S. Tarasov, M.L. Yanul
Ioffe Physical Institute; NT-MDT Co. & ITMO

Aperture SNOM applications (NT-MDT instrumentation)



Physical and chemical characterization at the nanoscale: experimental approaches utilizing AFM probe

➤ Co-localized AFM-Raman

- Comprehensive simultaneous physical (AFM) and chemical (Raman) sample characterization.
- Spatial resolution: AFM - ~ 1 nm; Raman - ~ 200 - 400 nm.
- Various excitation and collection geometries.

Controlled environment: liquid, gases,
temperature, electrochemistry, magnetic field

➤ Tip Enhanced Raman Scattering (TERS)

- Signal enhancement for weakly scattering samples.
- ~ 10 nm spatial resolution in Raman (chemical) imaging.
- Graphene and other carbon nanomaterials, polymers, thin molecular layers, semiconductor nanostructures, biological structures, DNA molecules etc.
- Advances in production of reproducible TERS probes (STM, tuning fork, AFM cantilevers).

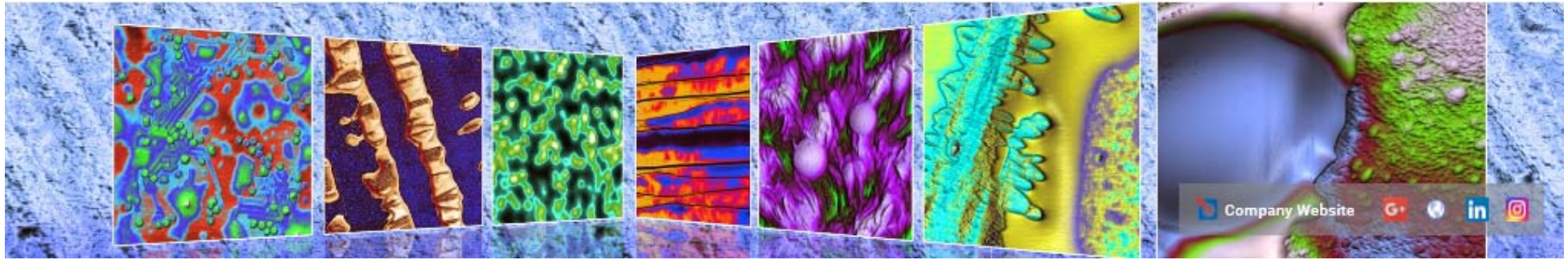
➤ Aperture scanning near-field optical microscopy (SNOM)

- $\sim \lambda/10$ spatial resolution (~ 100 nm for NIR).
- Advances in cantilever SNOM manufacturing: contact & non-contact probes, improved signal collection efficiency.
- Plasmonics and nanophotonics structures, lasers, optical fibers, photovoltaics, QDs, etc.



Thank you for your attention!

www.ntmdt-si.com



Follow us in social networks!
#NTMDT

